

FINAL REPORT

July 1991 through June 1994

FLANK SOLAR WIND INTERACTION

NASA Contract NAS5-31216

IN 92-CR

May 16, 1994

Principal Investigator: Stewart L. Moses

Co-Investigators: Eugene W. Greenstadt
Ferdinand V. Coroniti

Electromagnetic Systems and Technology Department, TRW

TRW Space and Electronics Group
Space and Technology Division
One Space Park
Redondo Beach, CA 90278

(NASA-CR-189327) FLANK SOLAR WIND
INTERACTION Final Report, Jul. 1991
- Jun. 1994 (TRW Space Technology
Labs.) 36 p

N94-35225

Unclas

G3/92 0014033

Technical Summary

Introduction

In this report we will summarize the results of the work performed under the "Flank Solar Wind Interaction" investigation in support of NASA's Space Physics Guest Investigator Program. While this investigation was focused on the interaction of the Earth's magnetosphere with the solar wind as observed by instruments on the International Sun-Earth Explorer (ISEE) 3 spacecraft, it also represents the culmination of decades of research performed by scientists at TRW on the rich phenomenology of collisionless shocks in space. For the opportunity to work in this field we are all indebted to the late Dr. Frederick L. Scarf.

The ISEE 3 spacecraft traversed many regions of unique importance to space physics during its long mission, and for this investigation we chose to examine several aspects of the solar wind interaction region on the far flanks of the bow shock. These studies encompassed the foreshock and magnetosheath as well as the shock itself. Most of our effort involved analysis of data from the ISEE 3 plasma wave investigation (PWS) [Scarf *et al.*, 1978], but also included correlative examinations of magnetometer [Frandsen *et al.*, 1978] and plasma analyzer data [Bame *et al.*, 1978].

The uniqueness of the solar wind interaction on the far flanks manifests itself in many forms. The primary reason for interest is that this region has seldom been encountered by spacecraft and the data obtained has been little analyzed. The ISEE 3 exploration of this region in 1982 and 1983 (prior to injection into a heliocentric orbit to intercept Comet Giacobini-Zinner) provided a valuable data set from a well-instrumented spacecraft. Other reasons for interest are intrinsic to the nature of the solar wind interaction at these distances downstream. Here the Mach number of the bow shock can become quite low, enabling us to investigate the transition from subcritical to supercritical shock fronts. We are also far from the leading edge of the foreshock, which allows us to observe the evolution of foreshock turbulence and attempt to distinguish upstream effects from phenomena that are integral with the shock structure. The geometry of this region is also different from that of the well-studied subsolar bow shock. On the dayside, the shock normal is nearly coaligned with the solar wind velocity, while on the flanks these two vectors are nearly orthogonal. This produces a second degree of freedom in the upstream shock parameters and also influences the trajectory of reflected particles parallel to the

shock surface. The low Mach number regime is also important because of the wealth of numerical simulations that have been performed in this parameter range and we have made use of these results for comparison with our spacecraft observations.

In the following sections we present our results organized by region: foreshock, shock and magnetosheath. Our studies have also supplemented related studies of shock physics in other areas (i.e. the solar corona) and we will also discuss these secondary contributions.

Foreshock

The extensive foreshock upstream of the Earth's bow shock, replete with turbulent plasma wave emissions, ULF magnetic field turbulence, and back-streaming particles, has been the subject of much study both to understand its intrinsic properties and to understand its relationship to the bow shock. In the subsolar region of the shock, for quasiparallel geometries, the foreshock and shock structures are intertwined as particles stream away from the shock and create foreshock turbulence which is blown back into the shock. On the far flanks we have a chance to try and view these effects decoupled, as the shock and foreshock leading edge are now far apart. We are also detecting shocks at Mach numbers near the limit where ion reflection begins to alter the magnetic field structure of the shock ramp. While the fluxes of reflected ions may be too small to produce noticeable magnetic field turbulence, they still have the potential to generate plasma waves. However, a new difficulty arises from the geometry of the far flanks, where the shock normal is now nearly orthogonal to the solar wind flow instead of coaligned.

As this research effort was getting underway, *Greenstadt et al.* [1991] presented an initial overview of the flank shock data set and compared the magnetic field profiles of several shocks with those found in weak, quasiparallel numerical shock simulations. These examples showed that even at low shock normal angles (θ_{Bn}) there was an absence of significant ULF turbulence upstream. However, there was often a pronounced whistler-like wavetrain either immediately upstream or downstream of the shock ramp. The simulations indicated that wavetrains only occurred when the Alfvén Mach number (M_A) exceeds 2.5, and this effect was corroborated in the flank shock data set. Clearly, this whistler-like wavetrain is a structure produced by the shock itself, while ISEE 3 was apparently too far downstream of the foreshock leading edge to detect strong ULF turbulence produced by foreshock particle populations. The nearly laminar appearance of

the quasiparallel flank shocks illustrated quite a contrast with the broad, turbulent quasiparallel shocks of the subsolar region.

Greenstadt et al. [1992a] set out to investigate in more detail the controlling factors in producing upstream particles by using broadband plasma wave emissions as a diagnostic of their presence. They found that these low Mach number shocks still produced copious amounts of plasma emissions upstream, but that the controlling factors were modified due to the unusual shock geometry on the flanks. A new parameter was introduced to aid in organizing the data-- θ_{Bx} , the angle between the IMF and the solar wind velocity (x in GSE coordinates). In the subsolar region θ_{Bx} and θ_{Bn} are nearly equal, but they vary independently on the flanks. For decreasing values of θ_{Bx} it was found that the extent of upstream plasma wave turbulence increased. *Greenstadt et al.* [1992a] concluded that this was caused by particles reflected upstream of the spacecraft location convecting back along the IMF with trajectories nearly parallel to the shock surface. Thus, nonlocal effects were shown to be important in the plasma waves, although not in the magnetic field, and upstream and reflected ion populations were still present without the ULF turbulence characteristic of the subsolar foreshock.

Greenstadt et al. [1992b] attempted to further define the contributions of θ_{Bx} and θ_{Bn} to the presence of upstream plasma wave turbulence by developing a scatter diagram showing the presence or absence of upstream waves. This ran into difficulties in distinguishing "foreshock" waves from "shock foot" waves. Subsequent analyses searched for additional parameters to aid in making this distinction, but adequate results were not forthcoming. A discussion of the work on employing plasma waves in detecting the presence of a shock foot appears in the next section.

ISEE 3 plasma wave data was also used to obtain a global view of the foreshock using a wave amplitude mapping scheme devised for Venus [*Crawford et al.*, 1993]. In this scheme, the wave amplitude in a particular channel is plotted as a function of its position in foreshock coordinates [*Greenstadt and Baum*, 1986] (distance along and depth behind the foreshock leading edge) to create a relief map of the wave activity independent of the orientation of the IMF. *Greenstadt et al.* [1993] presented a preliminary example of the results using one ISEE 3 trajectory through the foreshock and wave amplitudes corresponding to the electron plasma frequency (f_{pe}) and compared the resulting map with a similar one for Venus. At this stage the sampling spatial scale for Earth was still crude, since this employed data from only one Earth pass, while the Venus map was based on

thousands of PVO orbits. Yet, the terrestrial map showed the much greater scale of the Earth's foreshock compared with Venus and clearly delineated the enhanced wave activity in a thin band corresponding to the foreshock leading edge. This band of activity also had a definite termination near 100 Earth radii from the shock tangent point. Further analysis, unfinished at the time of this writing, will include a second ISEE 3 foreshock traversal. Line plots of intensity percentiles from both passes show pronounced maxima in median and higher intensities of wave peaks at, and just downwind from, the tangent IMF surface to the shock, much as in the Venus foreshock. It is hoped that this approach will be extended to include lower frequency waves associated with reflected ions. The foreshock defined by the low frequency plasma waves can then be compared with that defined by ULF structure in the magnetic field.

Shock

Greenstadt et al. [1992a] also addressed the problem of supercriticality in low Mach number shocks. The critical Mach number occurs when the shock can no longer create enough resistive dissipation, and must reflect a portion of the incoming ion flow. Theoretically this Mach number is defined as the point when the downstream flow speed exceeds the downstream acoustic speed as computed by the Rankine-Hugoniot relations. The usual way of identifying supercritical shocks is by the presence of a downstream "overshoot" and/or a "foot" to the shock ramp in the magnetic field profile. Some recent research has looked into the transition from sub- to supercritical shocks by searching for low fluxes of reflected ions in closed trajectories upstream of low Mach number shocks. The problem is naturally the ability to detect ion beams at low densities, but results indicate that the transition is not sudden and some reflected particles can be found even at the lowest Mach numbers.

Plasma waves can be even more sensitive to superthermal particle populations than direct particle detection, since they give rise to instabilities that cause the rapid growth of waves to detectable amplitudes. *Greenstadt et al.* [1992a] used the ISEE 3 flank shock data set as a source of low Mach number shock profiles and searched for a plasma wave foot immediately upstream of the shock ramp. It was found that most of the shocks were actually supercritical using the theoretical criterion given above, but one example was subcritical according to the Rankine-Hugoniot relations and many did not evidence a foot in the magnetic field profile. This ostensibly subcritical shock had a substantial plasma wave foot, showing that ion reflection was still taking place.

A more detailed study of the waves at and immediately downstream from the flank bow shocks was conducted by *Coroniti et al.* [1993]. The wave amplitudes at even the weakest shocks were found to be comparable with those found at high Mach number subsolar shocks. When examined at the highest time resolution, the plasma wave spectra revealed two modes in the mid-frequency band usually assigned to ion acoustic waves. Previous observations, concentrating on lower time resolution data or limited parts of the spectral band, identified only a single mode extending from approximately the electron cyclotron frequency (f_{ce}) to nearly the electron plasma frequency. The ISEE 3 results clearly show two modes with different temporal characteristics and quite independent of one another (the appearance of one mode is neither correlated or anti-correlated with the other).

The higher frequency mode is usually found between $1.0 - 0.1 f_{pe}$, and is distinguishable from narrowband electron plasma oscillations by its much broader bandwidth. These waves are found at frequencies above that expected for electrostatic waves Doppler-shifted by the solar wind and are outwardly similar to so-called "down-shifted" electron plasma oscillations detected deep within the foreshock [*Fuselier et al.*, 1985]. These emissions are strongly polarized parallel to the magnetic field. *Coroniti et al.* [1993] suggests that the instability generating these waves could arise from discontinuities in the electron distribution function. Such discontinuities would be the result of contact along the field lines between electron populations with different thermal characteristics. As electron populations encounter the cross-shock electric field, a void develops in the low energy region of the distribution function, which must be filled by scattering. With insufficient time to be relaxed through thermalization, the discontinuity in the electron distribution will produce an instability that can create waves at frequencies of a few tenths of the plasma frequency.

More of a mystery is the lower frequency emission, which occurs with a peak near the ion plasma frequency (f_{pi}) between 100 and 300 Hz. This mode is often separated from the higher frequency component by a pronounced spectral gap. Time series data shows that this emission is extremely bursty with peak to valley ratios of 100 to 1000 occurring in succeeding time samplings, unlike the smoother time profile of the high frequency emissions which only display a spin-modulated ripple of less than an order of magnitude. The burstiness of this emission renders polarization determinations difficult, but a slight parallel polarization can sometimes be discerned. It is also impossible to distinguish any

festooning effect caused by the response of the antennas to waves with wavelengths comparable to the antenna length [Gallagher, 1985]. What causes these waves is still not known. We do not observe any apparent frequency control by Doppler-shifting, although the absence of wideband data on ISEE 3 makes detailed spectral analysis difficult. The lack of any influence in the wave frequency by the value of the electron cyclotron frequency, which often occurs in this band, suggests an instability with k parallel to B . A parallel instability would more likely arise from variations in the electron distribution, but participation by the ions cannot be disregarded.

Magnetosheath

When observed from a global perspective, the magnetosheath has also been found to have new and interesting properties. Moses *et al.*, [1992a] presented long time series data showing several days of the ISEE 3 pass through the magnetosheath and foreshock. The sheath can be distinguished by the brightness of the broadband emissions there compared with the foreshock, even in the quasiparallel region. The sheath also contains electron plasma oscillations virtually throughout its extent toward the boundary with the tail lobe over $150 R_E$ downstream. This is quite surprising, since electron plasma oscillations are commonly considered a foreshock phenomenon.

The cause and nature of the broadband emissions far downstream of the bow shock are as yet unknown. Ion acoustic instabilities have been frequently invoked, but the difficulty of generating these emissions with the known ion temperatures has not been satisfactorily overcome. More needs to be learned about these emissions, and we have found a new factor controlling the emissions that could be fundamentally important in understanding their nature. A preliminary study [Moses *et al.*, 1993] and detailed follow-up [Coroniti *et al.*, 1994b] show that the direction of the magnetic field can have a significant effect on the presence or absence of wave emissions throughout the magnetosheath. Occasionally we noticed flank shocks without any waves at all immediately downstream and such dropouts were also observed much further inside the magnetosheath. During these times the wave amplitudes are reduced nearly to the instrument background. Surprisingly, these dropouts correspond to times when the component of the magnetic field parallel to the solar wind flow velocity (roughly the x -axis in GSE coordinates) goes to zero. No other factor seems to control the waves and the dropout effect occurs for any orientation of the magnetic field in the plane perpendicular to the flow. Occasionally a decrease in B_x also corresponds to a decrease in $|B|$, but this is not a prerequisite for a plasma wave dropout.

One reasonable explanation for this effect would be Doppler-shifting of low-frequency, parallel-polarized modes. The search for evidence of Doppler-shifting proved negative, however, as the peak frequency of the waves did not shift with intermediate values of the angle between the magnetic field and x (θ_{Bx}). The overall amplitudes do decrease in any given channel with intermediate values of θ_{Bx} suggesting that this parameter must influence the instability directly. We also do not observe an increase in amplitude with decreasing frequency, that would be indicative of Doppler-shifting.

The only hypothesis that seems consistent is that the direction of the magnetic field is controlling the nature of the connection of the field lines to the shock or magnetopause. This would determine the characteristics of the counter streaming electron populations that form the downstream distribution. When θ_{Bx} is 90° the shocks at either end of the field line are most likely to have similar properties (Mach number and shock normal angle), while other values of θ_{Bx} will lead to connection to shocks with differing characteristics. It is reasonable to assume that the symmetric case will lead to electron populations counterstreaming with nearly symmetric distributions, thus avoiding any discontinuities in the distribution function that would cause an instability. Connection to the magnetopause does not seem to be a factor, since this would only occur for large values of B_y . Although sketchy, this scenario is the only one that fits the phenomenology; however, its verification depends on detailed measurements of the electron distribution at low energies, which are difficult to obtain.

Related Studies

One of the original motivations at TRW to study the flank bow shock crossings was to apply the results to the ISEE 3/ICE encounter with Comet Giacobini-Zinner. *Smith et al.* [1986] used the Rankine-Hugoniot relations to argue that the crossings of the solar wind interaction regions of Giacobini-Zinner were low Mach number shocks, which was consistent with the arguments of *Scarf et al.* [1986] and *Kennel et al.* [1986] that the plasma wave phenomenology was indicative of shock crossings. These analyses were based on examinations of data on long timescales and other studies questioned the existence of an actual shock at Giacobini-Zinner. *Moses et al.* [1992] set out to examine the plasma wave data at the highest possible resolution (0.5 s) and compare the wave emissions with those found at weak flank shocks. At this resolution, it was hoped to be

able to associate various wave activity with ULF magnetic field turbulence which dominates the structure of the interaction region. No strong correlations between magnetic field structures and plasma wave spectra could be found, although the wave spectra tended to become more complicated (multi-peaked) as the magnetic field turbulence became more nonlinear. The high resolution analysis did show, however, that the same division between high frequency and low frequency emissions found in the flank shocks was evident in the comet waves. *Moses et al.* [1992] argued that the similarity in wave spectra probably arises from a similarity in microphysical processes in both cases. Thus the wave generation mechanisms at the comet are produced by the deceleration and compression of the solar wind associated with the ULF pulses (analogous to the processes in the ramp of a weak shock) and not by instabilities dependent directly on picked-up heavy ions.

In *Moses et al.* [1991] we applied some of the results from our low Mach number shock studies to conditions that could be encountered by a spacecraft penetrating the solar corona. Studies have been performed of missions designed to achieve heliocentric distances of 4 solar radii. At these distances magnetohydrodynamic models predict that the steady state solar wind is subsonic. But dynamic simulations show that low Mach number shocks could develop under extreme conditions. The closest analogy to such shocks in the corona would be quasiparallel bow shock crossings on the far flanks. We had earlier illustrated that even the lowest Mach number shocks on the flanks could produce magnetic field turbulence with $\delta B/B$ of order 1 and copious emissions of broadband plasma waves. Solar corona shocks would be in the slow mode (sub-Alfvénic) for $\beta \ll 1$ and not likely to produce large magnetic oscillations, but on the far flanks large amplitude turbulence was found even for $\beta = 0.4$. We therefore concluded that the solar corona could be expected to be extremely turbulent, with Doppler shifting caused by high spacecraft speeds to result in magnetic oscillation amplitudes of order Gauss at frequencies over 100 Hz. Again, using scaling arguments based on far flank shocks, we predicted electric field oscillations could attain amplitudes of order volts/meter at frequencies near 100 kHz. Such strong turbulence will also drive the plasma up to the Alfvén speed and produce nonthermal motions up to 200 km/s, which is near to the velocity fluctuations that have been deduced from radio scintillation and Lyman α measurements. To measure such wave activity would require specially designed instrumentation, with dynamic ranges and sensitivities drastically different from those previously flown.

Remarkably similar phenomenology to the flank shocks was also found in slow mode shocks on the boundaries of the plasma sheet in the distant magnetic tail [Moses *et al.*, 1992b; Coroniti *et al.*, 1994a]. As in the fast mode flank shocks, the broadband emissions in the slow mode shocks were found to be made up of two independent wave modes. The higher frequency mode also showed a strong parallel-polarization and exhibited a time profile modulated by a low amplitude spin-ripple. The low frequency modes were much burstier, with peak-to-valley ratios of 100 to 1000, and only a slight tendency toward parallel polarization. It thus appears that we are observing similar microphysical processes in distinctly different regions. Both the fast shocks and slow shocks have density compressions and the electron distributions in the parallel directions are controlled by the cross-shock electric field, but the magnetic field jumps, which should control the change in the perpendicular components of the distributions, are in opposite directions. This again points strongly to instabilities arising from free energy in the parallel component of the distribution.

Conclusions

The study of the solar wind interaction region on the far flanks has proven quite fruitful and has added to the understanding of processes in the foreshock, shock, and magnetosheath. We have discovered new wave modes and seen how different magnetic field geometries influence the presence and character of the waves. We have explored the important boundary between subcritical and supercritical shocks and mapped the global wave amplitudes in the foreshock. We have also applied the knowledge gained from the far flank shocks to the magnetotail, comets, and the solar corona. Much more can still be done both in exploring new phenomenologies and developing theories and models. This study, in a small way, shows the value of sustained research on existing data sets and the benefits of parallel investigations in related areas. Continued commitment to this mode of research, and support of well-established scientific teams, would have added to the advancement of scientific understanding in this field.

References

- Bame, S. J., J. R. Asbridge, H. E. Felthouser, J. P. Glore, H. L. Hawk, and J. Chavez, ISEE-C solar wind plasma experiment, *IEEE Trans., GE-16*, 160, 1978.

Coroniti, F. V., E. W. Greenstadt, S. L. Moses, E. J. Smith, and B. T. Tsurutani, Plasma waves downstream of weak collisionless shocks, *J. Geophys. Res.*, 98, 21,451, 1993.*

Coroniti, F. V., S. L. Moses, E. W. Greenstadt, B. T. Tsurutani, and E. J. Smith, Magnetic and electric field waves in slow shocks of the distant geomagnetic tail: ISEE 3 observations, in press, *J. Geophys. Res.*, 1994.**

Coroniti, F. V., E. W. Greenstadt, S. L. Moses, B. T. Tsurutani, and E. J. Smith, On the absence of plasma wave emissions and the magnetic field orientation in the distant magnetosheath, submitted to *Geophys. Res. Lett.*, 1994.*

Crawford, G. K., R. J. Strangeway, and C. T. Russell, VLF imaging of the Venus foreshock, *Geophys. Res. Lett.*, 20, 2801, 1993.

Frandsen, A. M. A., B. V. Connor, J. Van Amersfoort, and E. J. Smith, The ISEE-C vector helium magnetometer, *IEEE Trans.*, GE-16, 195, 1978.

Fuselier, S. A., D. A. Gurnett, and R. J. Fitzenreiter, The downshift of electron plasma oscillation in the electron foreshock region, *J. Geophys. Res.*, 90, 3935, 1985.

Gallagher, D. L. Short-wavelength electrostatic waves in the Earth's magnetosheath, *J. Geophys. Res.*, 90, 1435, 1985.

Greenstadt, E. W., and L. W. Baum, Earth's compressional foreshock boundary revisited: Observations by the ISEE 1 magnetometer, *J. Geophys. Res.*, 91, 9001, 1986.

Greenstadt, E. W., F. V. Coroniti, S. L. Moses, B. T. Tsurutani, N. Omid, K. B. Quest, and D. Krauss-Varban, Weak, quasiparallel profiles of Earth's bow shock: a comparison between numerical simulations and ISEE 3 observations on the far flank, *Geophys. Res. Lett.*, 18, 2301, 1991.**

Greenstadt, E. W., F. V. Coroniti, S. L. Moses, E. J. Smith, Plasma wave profiles of Earth's bow shock at low Mach numbers: ISEE 3 observations on the far flank, *J. Geophys. Res.*, 97, 10,841, 1992a.*

Greenstadt, E. W., S. L. Moses, F. V. Coroniti, and E. J. Smith, Plasma wave activity outside the far flanks of the Earth's bow shock, presented at the Spring Meeting of AGU, Montreal, Canada, May, 1992b.*

Greenstadt, E. W., S. L. Moses, F. V. Coroniti, G. K. Crawford, and R. J. Strangeway, Electron plasma oscillations in the foreshock: Comparison of occurrence at PVO and ISEE 3, presented at the Fall Meeting of AGU, San Francisco, December, 1993.*

Kennel, C. F., F. V. Coroniti, F. L. Scarf, B. T. Tsurutani, E. J. Smith, S. J. Bame, and J. T. Gosling, Plasma waves in the shock interaction regions at Comet Giacobini-Zinner, *Geophys. Res. Lett.*, 13, 921, 1986.

Moses, S. L., F. V. Coroniti, E. W. Greenstadt, and B. T. Tsurutani, Possible wave amplitudes in shocks in the solar corona: predictions for Solar Probe, *J. Geophys. Res.*, 96, 21,397, 1991.**

Moses, S. L., F. V. Coroniti, E. W. Greenstadt, and B. T. Tsurutani, Observations of plasma waves in the solar wind interaction region of Comet Giacobini-Zinner at high time resolution, *J. Geophys. Res.*, 97, 19,157, 1992.**

Moses, S. L., E. W. Greenstadt, F. V. Coroniti, and E. J. Smith, Plasma wave activity in the deep magnetosheath inside the far flanks of Earth's bow shock, presented at the Spring Meeting of AGU, Montreal, Canada, May, 1992.*

Moses, S. L., E. W. Greenstadt, F. V. Coroniti, and B. T. Tsurutani, Plasma waves in distant tail slow shocks, presented at the Fall Meeting of AGU, San Francisco, December, 1992.**

Moses, S. L., F. V. Coroniti, and E. W. Greenstadt, Magnetic field direction control of plasma wave emissions in the Earth's magnetosheath, presented at the Fall Meeting of AGU, San Francisco, December, 1993.*

Scarf, F. L., R. W. Fredricks, D. A. Gurnett, and E. J. Smith, The ISEE-C plasma wave investigation, *IEEE Trans.*, GE-16, 191, 1978.

Scarf, F. L., F. V. Coroniti, C. F. Kennel, D. A. Gurnett, W. -H. Ip, and E. J. Smith,
Plasma wave observations at Comet Giacobini-Zinner, *Science*, 232, 377, 1986.

Smith, E. J., et al., Analysis of the Giacobini-Zinner bow wave, *Eur. Space Agency Spec. Publ.*, ESA SP-250, (III) 461, 1986.

*Papers supported under this contract

**Related research papers

APPENDIX A

On the Absence of Plasma Wave Emissions and the Magnetic Field Orientation in the
Distant Magnetosheath. (Preprint)

On the Absence of Plasma Wave Emissions and the Magnetic Field Orientation in the Distant Magnetosheath

*F. V. Coroniti, E. W. Greenstadt, S. L. Moses
TRW Space and Electronics Group
One Space Park, Redondo Beach, CA*

*B. T. Tsurutani and E. J. Smith
California Institute of Technology
Jet Propulsion Laboratory
4800 Oak Grove Drive, Pasadena, CA*

Abstract. In early September, 1983 ISEE-3 made a long traversal of the distant dawnside magnetosheath starting near $x = -150 R_E$ downstream. The distant magnetosheath often contains moderately intense plasma wave emissions at frequencies from several hundred Hz to 5 kHz. However, over time scales of many days, a clear correlation exists between the occurrence of the plasma waves and the cone angle (θ_{xB}) between the magnetic field and the plasma flow velocity (x -direction). For θ_{xB} large (small), the plasma wave amplitudes are near background (high). Sudden (< 1 minute) changes in the local magnetic field orientation produce correspondingly sudden changes in the wave amplitudes. Statistically, the wave amplitudes decrease continuously with increasing θ_{xB} .

Introduction

Numerous observations from spacecraft have established that the Earth's bow shock excites a moderately intense band of plasma wave turbulence with frequencies between the ion and electron plasma frequencies (the so-called ion acoustic waves), which extends throughout the subsolar region of the magnetosheath [Rodriquez, 1978; Anderson et al., 1982; Onsager et al., 1989]. In September, 1983 the ISEE-3 spacecraft made a traversal of the distant dawnside magnetosheath starting about $x = -150 R_E$ and moving eastward [Greenstadt et al., 1990] and detected many long intervals of wave excitation in the flank sheath similar to that in the subsolar sheath even at these large distances from the bow shock. In addition, however, the ISEE-3 plasma wave instrument also detected many abrupt dropouts in the plasma wave emissions between the tail magnetopause and the flank bow shock. We report here for the first time these striking and rather curious

absences of plasma waves and their correlation with the orientation of the magnetosheath magnetic field.

Observations

The ISEE-3 measurements by the TRW/U. of Iowa electric field wave detector [Scarf *et al.*, 1978] and the JPL magnetometer [Frandsen *et al.*, 1978] presented here were made from 0000 to 1200 UT on both September 10 and 12 (days 253 and 255), 1983. During these intervals the spacecraft was continuously in the magnetosheath moving from $x = -158 R_E$, $y = -28 R_E$ to $x = -146 R_E$, $y = -33 R_E$ (GSE). The x-y projection of the spacecraft's trajectory for this sheath pass is shown in Figure 1. On September 10 (12), the magnetosheath flow speed varied from 500 to 600 km/s (400 to 500 km/s), the electron temperature was steady at 1.6×10^5 K, and the plasma density was in the range of 4 to 5 cm^{-3} (measurements from the LANL plasma analyzer). Figure 2 presents the measurements for September 12, 1983. The top panels display the 60-second average magnetic field components and magnitude. The central color panel presents the peak electric field amplitude (volts/meter) in the frequency channels from 100 Hz to 31 kHz which occurred during successive 60-second intervals. The next panel shows the magnetic field cone angle (θ_{xB})- the angle between the x-axis (nominal magnetosheath flow direction) and the magnetic field. The bottom two panels display the magnetic field longitude (defined so that 0° to 90° (-90° to 0°) corresponds to B_x and B_y having the same (opposite) signs), and the magnetic latitude.

Throughout this twelve hour interval plasma waves were almost continuously excited in the frequency band between 178 Hz and 3.1 kHz with the strongest signals occurring between 1.0 and 3.1 kHz. In addition intermittent bursts of electron plasma oscillations are evident in the 17 kHz channel. However, there are definite intervals of a few minutes duration when the peak electric field amplitude is near the background level of the wave instrument; clear examples are near 0020 UT, 0440 UT, 0650 UT, 0900 UT, and 1155 UT. In the magnetosheath and solar wind, the average (over 60 s) electric field amplitude can be near background while the peak amplitude will remain high; thus, a zero peak amplitude indicates the virtual absence of plasma waves.

The disappearance of the 178 Hz to 3.1 kHz wave emissions occurs when the magnetic cone angle exceeds 60° and is typically above 75° . From the top panels in Figure 2, large cone angles correspond to intervals in which B_x is small, while B_y and B_z have varying and comparable values. In particular the magnetic field latitude did not exceed 45° to 60° during the wave dropouts; since the ISEE-3 electric field antenna is in the ecliptic plane, a parallel polarized electric field signal will not be detected if the magnetic latitude was near 90° . The first four and sixth

dropouts occurred during small to moderate depressions in the magnetic field strength; however for the fifth and seventh dropouts, the field magnitude was steady.

Figure 3 presents the magnetic field and plasma wave measurements for 0000 - 1200 UT on September 10, 1983. From 0000 UT to 0400 UT and again from 0800 UT to 1200 UT, the magnetic cone angle was often near 90° or rapidly varied between 60° and 90° . Plasma wave emissions between 178 Hz and 3.1 kHz are virtually absent during these intervals except for brief isolated bursts which occur when the cone angle drops below 60° . Between 0420 UT and 0450 UT, the cone angle decreased to about 40° , and fairly continuous wave emissions developed. From 0600 UT to 0800 UT, the cone angle remained below 45° and strong plasma wave signals were detected; the continuity of the wave emissions was broken at 0715 UT by a brief increase of the cone angle to 80° . For this twelve hour period intermittent electron plasma oscillations at 17 kHz were present during intervals of both high and low cone angles, and their occurrence did not exhibit any clear correlation with the magnetic field direction.

Figure 4 presents higher resolution measurements for the interval 0150 UT to 0230 UT on September 12, 1983; the magnetic field is averaged over 3 seconds, and the electric field spectral amplitude is unaveraged with a resolution of 0.5 s. At 0154 UT the wave amplitudes drop to background as B_x decreases to approximately 1 nT and θ_{xB} increases above 60° . During the wave dropout, the field magnitude stays constant, B_y changes sign, and a strong $B_z > 0$ results in a high field latitude (approximately 70°). The wave dropout developed simultaneously in the frequency channels from 316 Hz to 3.1 kHz, and there was no evidence that the wave amplitudes swept downward (upward) in frequency as B_x decreased (increased). At 0200 UT, a sharp drop of B_x to near zero ($\theta_{xB} = 75^\circ$), again at constant field strength, produced a rapid decrease in the wave amplitudes. The cone angle remained high ($\theta_{xB} = 75$ to 90°) and wave amplitudes remained low from 0200 to 0208 UT, except for brief low frequency wave burst and $\theta_{xB} < 60^\circ$ dip at 0202:30 UT. Between 0208 and 0211 UT, θ_{xB} varied in the range 60° to 75° , and weak low frequency waves were observed. Except for a short burst at 0212 UT, these emissions terminated as B_x decreased to near zero at 0211 UT. From 0212 to 0220 UT, the field magnitude dropped to quite low values, B_x remained near zero, and all wave amplitudes were at background. At 0220 UT, the field strength recovered, B_x jumped to become the dominant field component, θ_{xB} decreased to 10° , and the 1.0 kHz to 3.1 kHz wave amplitudes started to increase. The wave amplitudes reached their previous (before 0154 UT) high levels after 0222 UT.

The temporal variations in the cone angle and plasma wave intensities on September 12, 1983 were sudden, radical changes from moderate to high θ_{xB} (Figure 2). Hence the question arises as to

whether the plasma wave amplitudes vary continuously with θ_{xB} or simply cut-off for angles above some threshold. Figure 5 presents a scatter plot of wave amplitude in the 1.78 kHz channel *versus* cone angle for the same time period shown in Figure 2 (the amplitudes indicate peak values in 1-minute intervals). The graph shows clear agreement with the general nature of the day's events, with most points at high intensity when θ_{xB} was usually below 40° and a much smaller number of points at low intensity, or instrument sensitivity limit, when θ_{xB} was less commonly above 50° . The apparent declining trend of intensity with angle, however, implies a continuous rather than "on/off" relationship between the two quantities for all angles. The wide scatter could be caused locally by several factors, such as the impulsive character of the plasma wave signals and the rapid fluctuations of the cone angle.

Discussion

The above examples have clearly demonstrated that in the distant dawnside magnetosheath the occurrence of plasma waves in the 316 Hz to 3.1 kHz band is associated with the local magnetic field direction. This relationship held for the entire dawnside pass shown in Figure 1. We have also observed the same anti-correlation between wave amplitude and high values of θ_{xB} in the duskside magnetosheath, but not in the upstream solar wind. The anti-correlation is so distinct that the first inclination is to seek an instrumental explanation. The ISEE-3 antenna is in the ecliptic plane, and thus electric fields which are perpendicular to the ecliptic are not measured. However, even if the waves were polarized exactly parallel to the magnetic field, which is not at all clear or even likely, the large cone angles, which imply B_x was small, usually occurred when B_y was quite finite so that the magnetic field latitude did not exceed 45° to 60° ; therefore, the cosine reduction in the projected measured field amplitudes cannot explain the virtual disappearance of the wave emissions.

If the wave polarization is strongly field-aligned, another conceivable explanation involves the Doppler shift frequency $\omega_D = \mathbf{k} \cdot \mathbf{v}$, which would vary as $\cos\theta_{xB}$. If the observed frequencies are dominated by ω_D , the reduction of $\cos\theta_{xB}$ would shift the peak spectral amplitude to lower frequencies; thus on the higher frequency, falling part of the spectrum, the amplitudes would decrease, and the waves would appear to drop-out. However, in examining the temporal behavior of the amplitudes in the various frequency channels during changes in θ_{xB} (as in Figure 4), the spectral peak does not shift to lower (higher) frequencies as θ_{xB} increases (decreases). Hence we conclude that the dropouts are not due to θ_{xB} variations in the Doppler shift frequency.

The absence of an instrumental or Doppler shift explanation leaves the possibility that the wave emissions are controlled by parameters not included in this report or by the global connection of the magnetic field to the bow shock and/or magnetosphere. Since ISEE-3 was within 20-30 R_E of the tail magnetopause, the local magnetosheath field lines could be influenced by the location, shape, and/or reconnection state of the magnetotail. We have checked on whether the plasma wave dropouts and turnons depend on the signs of B_y and B_z , which could indicate a sensitivity to reconnection-related magnetotail structure and B_y -twist of the tail's orientation, and found no obvious relation. Since dropouts occur when $B_y = 0$, the intersection of the field lines with the magnetotail is not essential to produce the amplitude decreases. Thus we conclude that the wave dropouts are not obviously produced by connection to the magnetosphere.

The wave dropouts can persist for many minutes to hours, which indicates that the large scale structure of the magnetic field, not the small scale or local wiggles, is responsible for the absence of wave emissions. When θ_{xB} is large, the nose region bow shock is in a quasiperpendicular configuration over most of the region sunward of the terminator. Thus most of the magnetosheath ions which flowed past the ISEE-3 spacecraft on September 10 and 12, 1983 crossed a quasiperpendicular shock, and thus might be expected to possess at least the remnants of a reflected ion or ring-type phase space distribution. Downstream of the terminator, the field lines would typically intersect the weak flank shock surface in the quasiparallel configuration. Since the magnetosheath electrons (ions) have thermal speeds of about 20 R_E /min (0.5 R_E /min) the local electrons (ions) would (not) have passed through a quasiparallel shock. Furthermore the shock strength at the two intersection points of the field line would be about equal, so that the distribution function of the shocked electrons would tend to be symmetric with respect to the parallel velocity. Thus the absence of plasma waves when θ_{xB} is large may be caused by the symmetry of the electron distribution in parallel velocity even if the local ion distribution contains remnants of the ring-type structure produced by ion reflection.

When θ_{xB} is small, the dawnside shock in the nose region is quasiparallel (quasiperpendicular) if the magnetic field is in a Parker (anti-Parker) spiral configuration. We found that the plasma wave emissions in the distant magnetosheath occur independently of the relative sign between B_x and B_y ; thus the waves are present for local magnetosheath ion distributions which have passed through either a quasiparallel or quasiperpendicular shock. For small θ_{xB} , both the shock strengths and shock type at the two locations where the magnetic field line intersects the shock surface are very different. Thus the local electron distribution, which is in thermal contact with the bow shock, is likely to be asymmetric with respect to the parallel velocity.

In conclusion, one identified explanation we have been unable to eliminate for the observed anti-correlation of θ_{xB} and plasma wave emissions is that when θ_{xB} is small, the expected asymmetry in the local electron distribution leads to plasma wave excitation, and when θ_{xB} is large, the field line connection to similar strength and type bow shocks results in a more symmetric electron distribution which is stable to wave emissions. Clearly GEOTAIL electron and ion plasma measurements will be able to test this possible explanation and/or provide a better one.

Acknowledgments

We acknowledge and pay homage to the late F. L. Scarf, the original Principal Investigator for the ISEE-3 plasma wave investigation, who made possible our participation in the study of plasma waves in space. The work at TRW was supported by NASA Contract NAS5-31216 with GSFC. The work at the California Institute of Technology, Jet Propulsion Laboratory was supported by contract with NASA.

References

- Anderson, R. R., C. C. Harvey, M. M. Hoppe, B. T. Tsurutani, T. E. Eastman, and J. Etcheto, Plasma waves near the magnetopause, *J. Geophys. Res.*, *87*, 2087, 1982.
- Frandsen, A. M. A., B. V. Connor, J. Wan Amersfoort, and E. J. Smith, The ISEE-C vector helium magnetometer, *IEEE Trans.*, *GE-16*, 195, 1978.
- Greenstadt, E. W., D. P. Traver, F. V. Coroniti, E. J. Smith, and J. R. Slavin, Observations of the flank of Earth's bow shock to $-110 R_E$ by ISEE 3/ICE, *Geophys. Res. Lett.*, *17*, 753, 1990.
- Onsager, T. G., R. H. Holzworth, H. C. Koons, O. H. Bauer, D. A. Gurnett, R. R. Anderson, H. Luhr, and C. W. Carlson, High frequency electrostatic waves near Earth's bow shock, *J. Geophys. Res.*, *94*, 13,397, 1989.
- Rodriquez, P., Magnetosheath electrostatic turbulence, *J. Geophys. Res.*, *84*, 917, 1979.
- Scarf, F. L., R. W. Fredricks, D. A. Gurnett, and E. J. Smith, The ISEE-C plasma wave investigation, *IEEE Trans.*, *GE-16*, 191, 1978.

Figure Captions

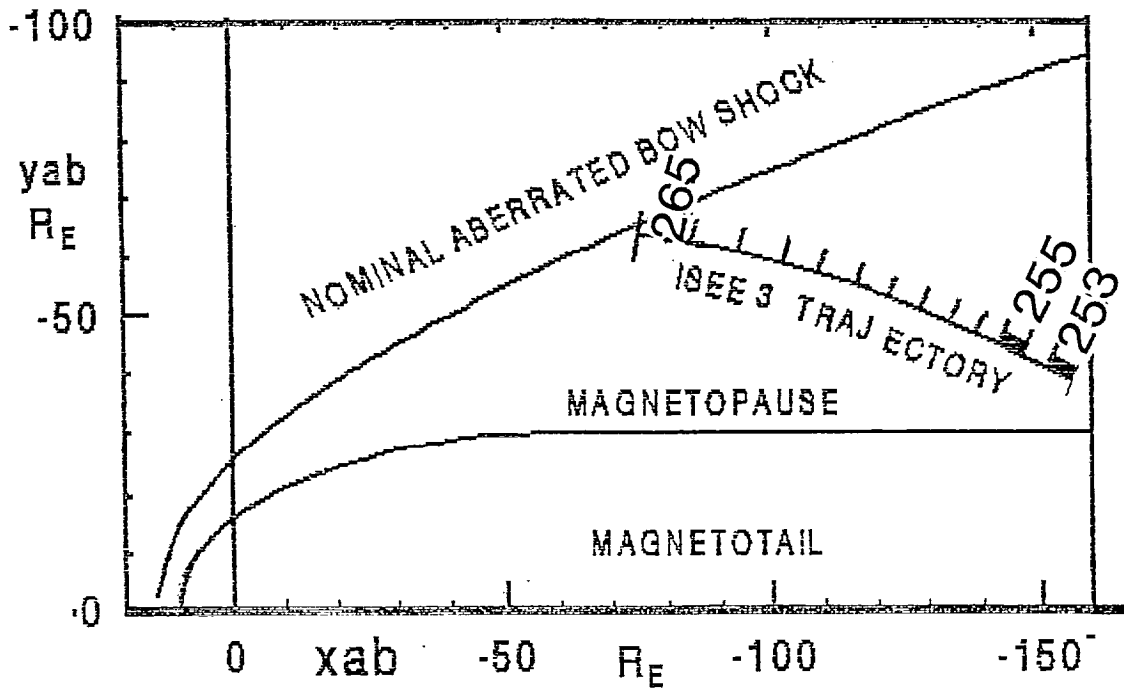
Figure 1. ISEE 3's magnetosheath trajectory for days 253-265, 1983. The heavy segments represent 10 and 12 September, when the spacecraft was approximately 17-18.5 R_E above the x-y plane.

Figure 2. ISEE-3 measurements on 0000 UT to 1200 UT on September 12, 1983. The upper panels present the one-minute average components and magnitude of the magnetic field. The center panel is a color-coded display of the plasma wave electric field amplitudes (volts/m) from 100 Hz to 31.6 kHz. The bottom panels present the calculated magnetic field cone angle (θ_{xB}) and the longitude and latitude of the field as defined in the text. Clear dropouts in the plasma wave amplitudes occur when θ_{xB} approaches 90° .

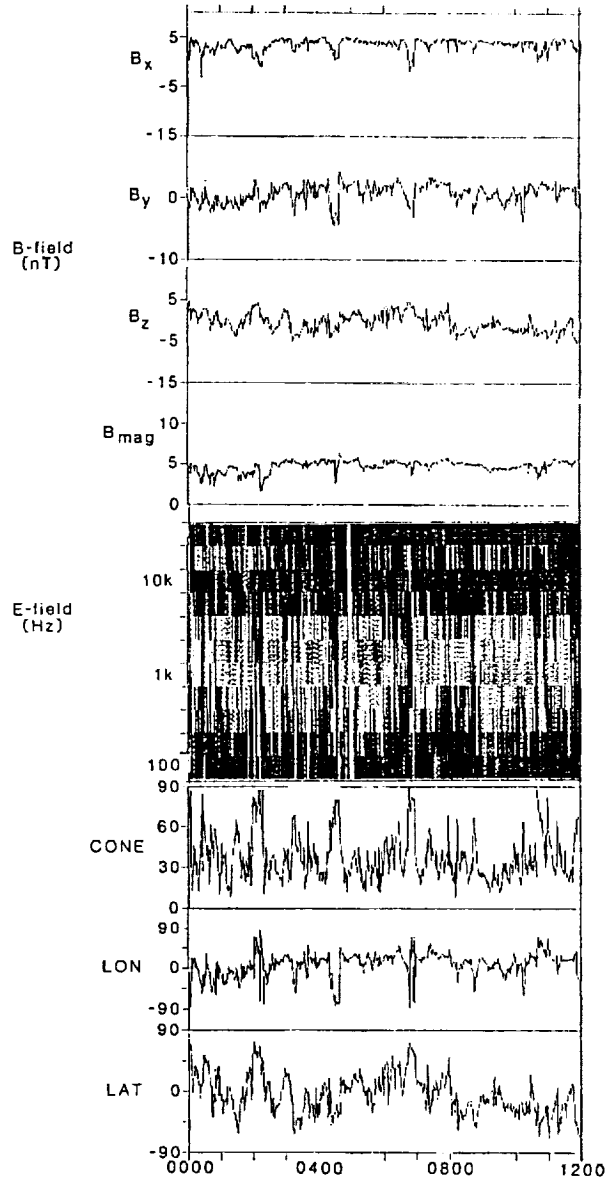
3. ISEE-3 measurements on 0000 UT to 1200 UT on September 10, 1983, in the same format as Figure 2. Plasma wave amplitudes are high only when the cone angle is below 40° .

Figure 4. High time resolution measurements from 0150 UT to 0230 UT on September 12, 1983. The bottom (top) panels display the measured (calculated) magnetic field components and magnitude (magnetic angles). The center panel shows the plasma wave spectral amplitude from 178 Hz to 3.16 kHz. Sudden changes in θ_{xB} result in sudden changes in the wave amplitudes.

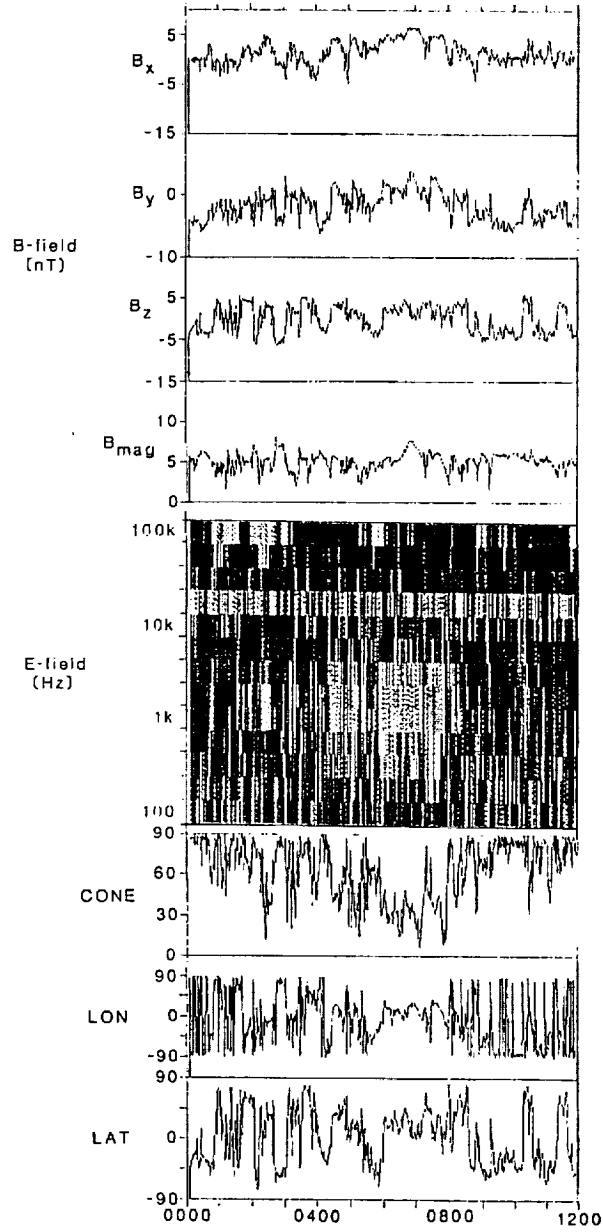
Figure 5. A scatter plot of the plasma wave electric field amplitude (volts/m) *versus* cone angle for the 0000 - 1200 UT interval on September 12, 1983. Although the scatter is large, the decrease of wave amplitudes with increasing cone angle is clear.



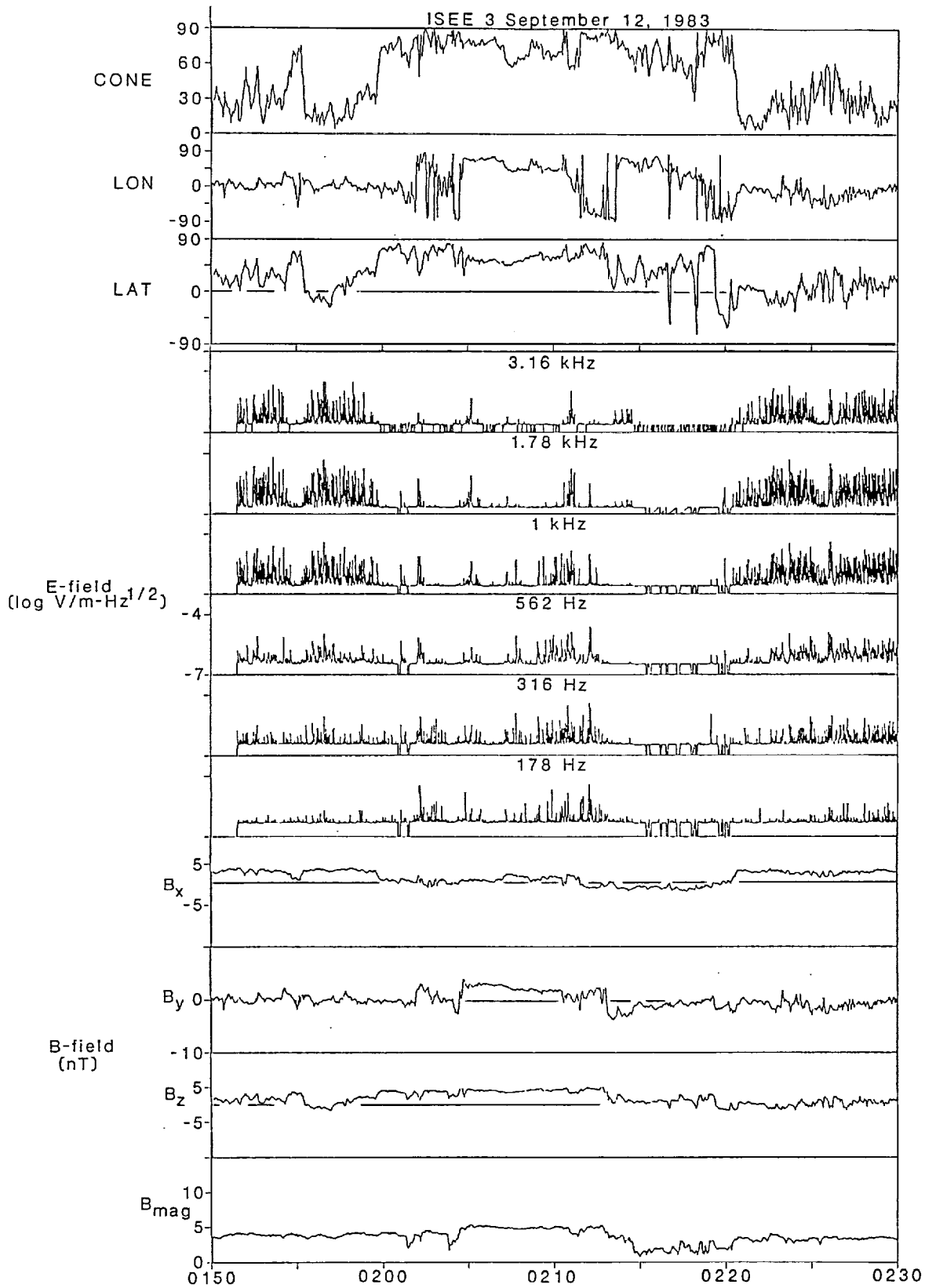
ISEE 3 September 12, 1983



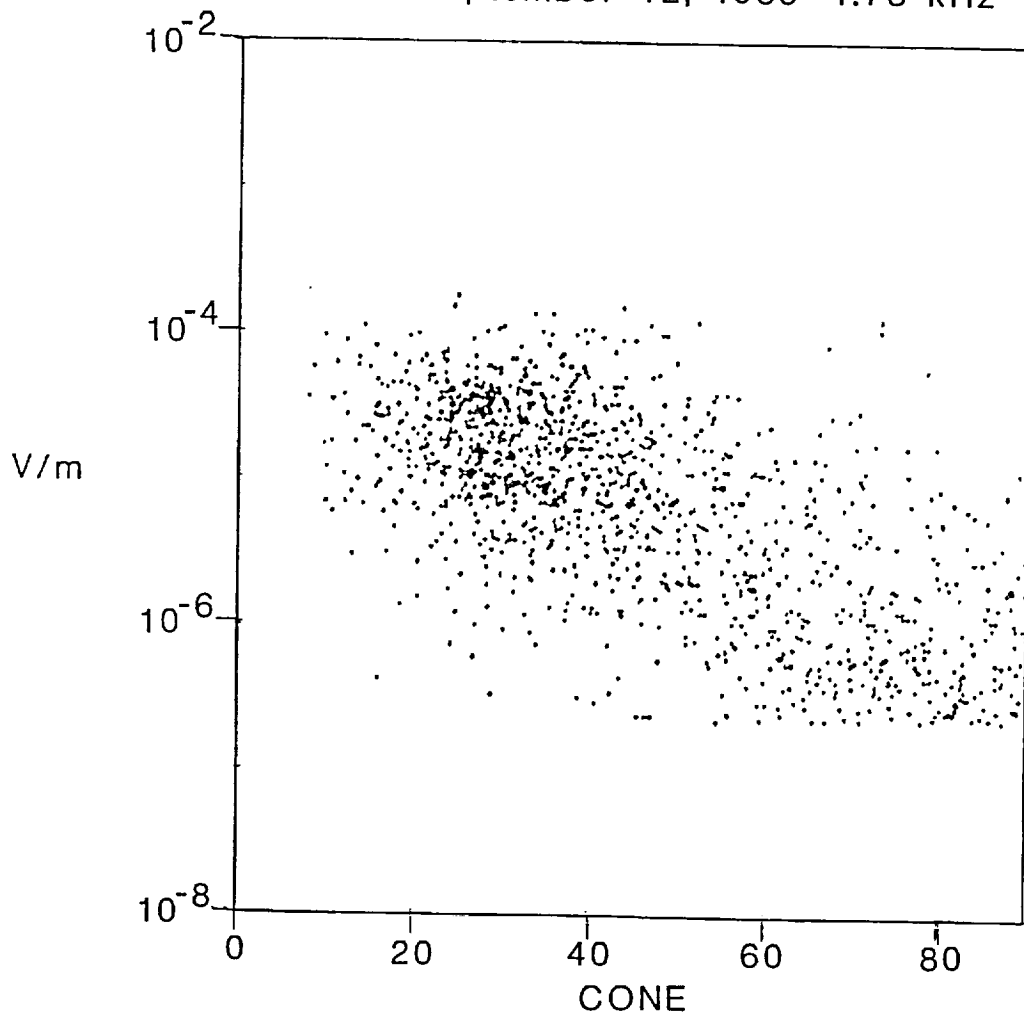
ISEE 3 September 10, 1983



ISEE 3 September 12, 1983



ISEE 3 September 12, 1983 1.78 kHz



APPENDIX B
Abstracts and First Pages of Publications

WEAK, QUASIPARALLEL PROFILES OF EARTH'S BOW SHOCK:
A COMPARISON BETWEEN NUMERICAL SIMULATIONS
AND ISEE 3 OBSERVATIONS ON THE FAR FLANK

E. W. Greenstadt¹, F. V. Coroniti¹, S. L. Moses¹, B. T. Tsurutani²
N. Omid³, K. B. Quest³, and D. Krauss-Varban³

Abstract. Over 200 crossings of the distant downwind flanks of Earth's magnetosonic bow shock by ISEE 3 included many cases of weak, or low Mach number, quasiparallel shocks. A consistent feature of the magnetic field profiles was the presence of large amplitude, near periodic to irregular transverse oscillations downstream from even the weakest Q_{\parallel} shocks. Large downstream perturbations with whistler-like features similar to those of the observations appear in one-dimensional simulations when $M_A > 2.5$ but not when $M_A = 2.1$. The observed cases with downstream waves also occurred when $M_A > \approx 2.5$, suggesting the importance of the Alfvén as opposed to magnetosonic Mach number in determining the signature of weak, Q_{\parallel} shocks.

Introduction

We present observations of weak, quasiparallel bow shocks exhibiting large amplitude, downstream oscillations compatible with those of new numerical simulations of quasiparallel shocks that, although weak (low magnetosonic Mach numbers M_{MS}), have moderate Alfvén Mach numbers (M_A) and downstream wavetrains. The terms quasiparallel (Q_{\parallel}) and quasiperpendicular (Q_{\perp}) refer to planar shocks whose normal makes an angle $\theta_{bn} < 45^\circ$ or $> 45^\circ$ from the upstream field B_1 . We use the term "weak," rather than "low Mach number," to describe the shocks of interest here. No local plasma ion data from which to approximate magnetosonic Mach numbers M_{MS} were available from ISEE 3 at the time of the flank observations. Estimates of magnetosonic Mach numbers would have to assume a "typical" ion temperature, say $T_i = T_e/2$, and project the approximate solar wind electron velocities along the local normals. However, the upstream solar wind's electron parameters can be determined only when the spacecraft was outside the shock, so the instantaneous projected velocities, hence projected Mach numbers, especially for crossings that exit the magnetosheath, cannot be certain, and the speed of the shock itself, also necessary for determining its instantaneous Mach number, is unknown from ISEE 3's single-spacecraft crossing times. Instead of instantaneous Mach numbers, we have adopted the ratio of downstream to upstream field magnitudes $M_B = B_2/B_1$ as a measure of shock strength approximating the true Mach number in Q_{\perp} , but underestimating it in Q_{\parallel} , geometry [Kennel et al., 1985]. In many of the over 200 flank crossings, M_B has been found to be the same or within one or two tenths of the projected M_{MS} , supporting the adoption of M_B as a practical tool for estimating shock strengths--with appro-

priate caution. Regardless of these generalized caveats, the observed and numerical examples in this report had comparable values of M_B .

We describe the observational context of weak, Q_{\parallel} shocks and our sources of shock data, present examples illustrating the unusual natural wave signatures, compare them with new simulation results, and discuss the outcome for the first few selected cases.

Context

The small sampling of naturally occurring weak, Q_{\perp} shocks previously reported has produced some surprising results, most notably evidence of reflected, nonlaminar ion populations [Bavassano-Cattaneo et al., 1986; Greenstadt and Mellott, 1987] and ion heating [Thomsen et al., 1985]. With renewed interest in weak shocks, simulators as well as observers have independently been extending their results toward the less documented classes of Q_{\parallel} and weak shocks, especially the rarely recorded weak, Q_{\parallel} combination [Mandt et al. 1986; Omid et al. 1990].

Until recently, the largest number of weak, Q_{\parallel} shocks recorded by satellite was a subset of interplanetary events encountered by ISEE 1,2,3 [Tsurutani et al., 1983; Russell et al., 1983] and Helios [Richter et al., 1986]. High resolution profiles were described by Tsurutani et al. and Russell et al., who found their examples populated by two kinds of precursors in low and high Mach number cases ($M > 1.5$): regular, near periodic oscillations of the character of whistler mode waves (at low M), and irregular, broadband waves of linear polarization, whose amplitudes increased in Q_{\parallel} geometry (at high M). The whistlers occurred solely upstream from their corresponding shocks; the irregular waves appeared both up- and downstream from the shocks, and were seen to be larger downstream. Later, Mandt et al. attempted to simulate the interplanetary examples of Russell et al. case by case. Their profiles mimicked the appearance of an upstream whistler case, and also showed some additional irregularity in the profiles of other cases, albeit without the enhancement of wave amplitudes downstream, but tended to exhibit relatively regular waves in all examples. Both observed and simulated whistlers led from upstream into, but never further than, the tops of the shock ramps.

Lately, Omid et al. [1990] ran numerical experiments on weak, Q_{\parallel} shocks using a hard reflecting wall to form the shock. Their simulations produced two types of upstream wavetrains: initially phase standing dispersive whistlers, subsequently replaced near the shock by larger amplitude, longer wavelength whistlers. These later waves were generated by a resonant ion beam instability with group speed $V \approx 2.5V_A$.

ISEE 3 frequently recorded Q_{\parallel} crossings along the distant flank with trains of large, primarily transverse oscillations downstream from the clear shock jump in the field magnitude, but with an almost total absence of such oscillations upstream, in contrast with earlier observations and with the Omid et al. [1990] simulation. We therefore searched for bow shock examples whose plasma parameters were close to those of the simulations and looked for simulation profiles that might imitate the examples.

¹TRW, Inc., Redondo Beach, CA

²Jet Propulsion Laboratory, Pasadena, CA

³University of California at San Diego, La Jolla, CA

Copyright 1991 by the American Geophysical Union.

Paper number 91GL02246
0094-8534/91/91GL-02246\$03.00

POSSIBLE WAVE AMPLITUDES IN SHOCKS IN THE SOLAR CORONA:
PREDICTIONS FOR SOLAR PROBE

S. L. Moses, F. V. Coroniti, and E. W. Greenstadt

TRW Space and Technology Group, Redondo Beach, California

B. T. Tsurutani

Jet Propulsion Laboratory, California Institute of Technology, Pasadena, California

Abstract. Shocks and Alfvén turbulence are frequently invoked as mechanisms to heat the solar corona and accelerate the solar wind. A primary objective of the Solar Probe Mission is to detect and characterize these nonthermal dissipation and energization processes. Although the solar wind in the corona is usually assumed to be sub-Alfvénic, temporal and spatial variability in the plasma parameters could lead to conditions under which weak, fast mode shocks might form. ISEE 3 data from the flanks of the Earth's bow shock show that even low Mach number, quasi-parallel shocks generate large-amplitude Alfvén turbulence with $\delta B/B$ of the order of 1, and intense high-frequency electrostatic plasma waves. Using a model of the corona and scaling parameters to those expected in the regions to be traversed by Solar Probe ($r \geq 4 R_S$), we suggest it is possible that such shocks might produce Alfvén turbulence with magnetic field amplitudes up to the order of 0.1 G and electric field amplitudes up to the order of 1 V/m; electrostatic waves near 100 kHz may have amplitudes of 0.1 V/m. Since the shock-generated Alfvén waves would be Doppler shifted to frequencies of a few kilohertz because of the high spacecraft velocity at perihelion, detection of these waves imposes severe requirements on the designs of plasma wave and magnetic field sensors on Solar Probe.

1. Introduction

Determination of the physical processes which heat the solar corona and accelerate the solar wind is a major objective for the planned Solar Probe Mission. Many of the proposed coronal heating and acceleration mechanisms involve interactions with magnetohydrodynamic (MHD) waves and shocks (a thorough review is given by Narain and Ulmschneider [1990]). Very low frequency Alfvén waves may be generated by the 5-min photospheric oscillations and/or convection turbulence [Hollweg, 1983]. Coronal shocks can be excited by impulsive mass flows, diverging flow geometries, and/or local momentum addition [Habbal and Tsinganos, 1983]; such shocks are expected to have low Alfvén Mach numbers and to be in the quasi-parallel regime. These theories are supported by observational evidence of turbulence in the solar corona. Withbroe et al. [1985] analyzed Lyman α emissions in the region $2.8-4 R_S$ and found evidence for nonthermal motions with velocities $\delta v = 50-90$ km/s. Radio scintillation measurements indicate a peak in the coronal random motions of $\delta v = 200$ km/s near $10 R_S$ [Ekers and Little, 1971; Coles et al., 1978].

Within $10 R_S$ the solar wind in the corona is normally assumed to be sub-Alfvénic and low β . Therefore standing weak shocks should be on the slow mode branch and are unlikely to produce much hydrodynamic wave turbulence. Propagating fast mode shocks could be driven by rapid changes in the configuration of the lower corona, and these shocks could exceed the critical

switch-on Alfvén Mach number, above which shocks are expected to excite large-amplitude Alfvén turbulence. In any case, much is still not known about coronal plasma parameters, particularly on small scales, and it may be reasonable to expect that local temporal and spatial variations may produce weak, fast shocks. However, the primary purpose of this paper is neither to debate the existence nor to explore the physical consequences of weak, fast shocks in the solar corona, but to point out that in attempting to measure the properties of such shocks, the Solar Probe instrumentation will be severely tested. At Earth, low Mach number, quasi-parallel shocks generate large-amplitude, high-frequency Alfvén turbulence and intensive plasma wave emissions, and we suggest that similar shocks might produce extended regions of large-amplitude Alfvén and plasma wave turbulence in the solar corona. In this paper we scale the terrestrial shock measurements to coronal parameters, and we argue that in order to properly characterize such phenomena, significant improvements on current instrument designs will be necessary for Solar Probe.

In section 2 we present one particular model of coronal shock formation to obtain an estimate of likely shock parameters. Section 3 presents cases from the ISEE 3 crossings of the far flanks of the Earth's bow shock that fit these parameters and discusses the character of the wave activity found downstream. In section 4 we scale the turbulence in the magnetosheath to predict the amplitudes and frequencies of wave emissions in the regions to be encountered by Solar Probe. In section 5 we discuss the impact of these results on the scientific requirements of the Solar Probe mission, and this is followed by a brief summary.

2. Coronal Shocks

Kopp and Holzer [1976] showed that additional critical points can appear near the base of the corona when the rate of divergence of flux tube area with increasing radial distance is greater than r^2 ; Holzer [1977] extended this result by showing that additional points could also be obtained by localized heat and momentum addition to the flow. For flows with multiple critical points, Habbal and Tsinganos [1983] proposed that shocks could develop in the solar wind flow; later Habbal and Rosner [1984] and Habbal [1985] found solutions involving standing shocks in the near-Sun solar wind flow. Recently Leer and Holzer [1990] have argued that standing shocks are extremely unlikely for the plasma parameters expected in coronal holes. However, smaller-scale structural variability in either the magnetic field configurations or the plasma parameters might produce shocks, which need not stand in the solar wind flow but propagate in the corona.

Figure 1 presents some results from hydrodynamic simulations of the solar corona contained in Figure 3 of Habbal and Rosner [1984]. Each of the panels in Figure 1 depicts the density profile of the solar wind within $6 R_S$. The top panel shows the steady state configuration which develops when momentum is applied to the flow gradually (rise time of 2×10^4 s) and creates a standing shock. The magnitude of the density jump of this shock, n_2/n_1 , is approximately 2. The middle panel shows a

Copyright 1991 by the American Geophysical Union

Paper number 91JA02268.
0148-0227/91/91JA-02268\$02.00

to quasi-parallel. In the supercritical regime we examine how the overshoot evolves with the shock normal angle, and finally, for both subcritical and supercritical shocks, we examine the effect of the interplanetary field direction on the magnitude and structure of the non-coplanarity component of the magnetic field in the shock ramp.

SH41A-5 0830h POSTER

Unusually Distant Bow Shock Encounters at Times of Very Low Mach Number

T L Zhang (Space Research Institute, Graz, Austria)
C T Russell (Institute of Geophysics and Planetary Physics,
University of California Los Angeles, Ca 90024-1567; 310-825-3188; Internet crussell @ ipp.ucla.edu)

The distance of the bow shock from a planetary obstacle is determined by the compressibility of the plasma and the Mach number of the flow. When the Mach number is low the plasma is only weakly compressed and the shock must move away from the planet in order for all the shocked plasma to move around the planet. Spreiter et al. [1966] provided a simple relationship for this standoff distance for gasdynamic flows in terms of the Mach number at infinity and the polytropic index and tested it for Mach numbers from 5 to 100. We have examined Pioneer Venus data at times when the interplanetary magnetic field is strong and as a consequence the magnetosonic Mach number approaches unity. At these times the Venus bow shock becomes very dynamic and is encountered far upstream of its expected location, based on the earlier gasdynamic simulations at higher Mach numbers. These observations indicate that it is important to extend the simulations, particularly MHD simulations to lower Mach numbers. Also caution should be used in interpreting distant bow shock locations as evidence for planetary magnetic fields when the Mach number of those distant shocks is unknown.

SH41A-6 0830h POSTER

Analysis of the Neptune Bow Shock

A Szabo (MIT Center for Space Research, Cambridge, MA 02139)

R. P. Lepping (NASA Goddard Space Flight Center, Code 692, Greenbelt, Md 20771)

During Voyager 2's approach to Neptune, the spacecraft crossed a high Mach number ($M = 26$) and high β ($\beta = 6$) bow shock. Preliminary calculations (Szabo et al., A.G.U. Abstract Spring 1991 Meeting, EOS April 23, 1991.) depended on the assumption of a perpendicular shock normal to the local interplanetary magnetic field (IMF). Using the non-linear least squares technique of Vinas and Scudder (Vinas and Scudder, *J. Geophys. Res.* 92, 39, (1986)), we determined that the angle between the bow shock normal and the IMF as $84^\circ \pm 8^\circ$, validating the previous assumption. Also the bulk motion of the shock was determined to be 15 ± 10 km/s moving away from the planet, towards the Sun. With the knowledge of the bulk speed of the shock, the scale length of the foot and ramp of the shock can be calculated and compared with theoretical values. Similarly, the asymptotic plasma and magnetic field parameters are obtained showing a good agreement with the idealized Rankine-Hugoniot shock jump conditions.

The same in depth analysis is carried out for the outbound crossings of the Neptune bow shock. In addition, all of the Neptune results are compared to the newly evaluated Uranian shock parameters.

This work supported in part by NASA contract 76294.

SH41A-7 0830h POSTER

Highly Structured Langmuir Wave Emissions Observed Upstream of the Venesian Bow Shock

G B Hospodarsky, D A Gurnett, W S Kurth, (Department of Physics and Astronomy, University of Iowa, Iowa City, IA 52242; 319-335-1696; SPAN: IOWAVE::Hospodarsky)
S J Bolton (JPL, Pasadena, CA), M Kivelson, and R Strangeway (both at UCLA, Los Angeles, CA)

A series of highly structured Langmuir waves produced by energetic electrons streaming into the solar wind from the Venesian bow shock have been captured using wideband electric field measurements on the Galileo spacecraft during the flyby of Venus on February 10, 1990. The wideband sampling system on Galileo provides digital electric field waveform measurements at sampling rates up to 201,600 samples per second. This data provides much higher resolution waveform measurements than any previous instrument of this type. The main Langmuir wave emission occurs near the local electron plasma frequency, which was approximately 43 kHz. Large downshifts and upshifts in the emission frequency are observed, sometimes by as much as 20 kHz. The downshifts are correlated with the downstream distance from the magnetic field line tangent to the bow shock. The Langmuir wave bursts have a great deal of fine structure, with many intense bursts observed on time scales as short as one millisecond, corresponding to spatial scales of a few tens of Debye lengths. The origin of the fine structure and the shifts in frequency will be discussed.

SH41A-8 0830h POSTER

Strong Langmuir Turbulence in Jupiter's Foreshock?

Iver H Cairns (Department of Physics and Astronomy, University of Iowa, Iowa City, IA 52242; 319-335-1696; CAIRNS@IOWAVE.PHYSICS.IOWA.EDU)

Peter A Robinson (School of Physics and Research Center for Theoretical Astrophysics, University of Sydney, NSW 2006, Australia)

While Langmuir waves are observed in all planetary foreshocks, there is no theoretical consensus on the nonlinear processes limiting the wave growth. One significant difficulty involves Gurnett et al.'s [JGR, 86, 8833, 1981] Langmuir wave packets with very small scale sizes $\sim 100\lambda_e$ in Jupiter's foreshock. Although reminiscent of strong turbulence collapse, Gurnett et al. could not prove that the waves packets met the collapse threshold. Strong turbulence theory has progressed significantly in recent years. Here we assess whether Gurnett et al.'s observations are consistent with the new nucleation scenario for Langmuir wave collapse. Theoretical constraints on the fields and scale sizes of collapsing wave packets are summarized and placed in a form suitable for easy comparison with Voyager and Ulysses data. A new constraint is developed for collapse in the presence of background density fluctuations that disrupt the wave packet. The following conclusions are reached following review of the published data and instrument characteristics. (1) Wave packets formed from the observed large-scale fields cannot collapse if formed at the nucleation scale because they are disrupted before they can collapse. (2) Strict constraints on the wave packet fields exist; $E(L < 1000\lambda_e) \geq 1 \text{ mV m}^{-1}$, even if a new formation process can be found. (3) The published wave packets have fields much smaller than those required for collapse. (4) Collapse remains possible for at most a fraction of wave packets. (5) Explanations other than strong turbulence collapse must apply to the majority of observed wave packets. Means for testing these conclusions using Voyager and Ulysses data are suggested.

SH41A-9 0830h POSTER

A Study of Langmuir Waves Upstream from Uranus' Bow Shock

S Xue, I H Cairns, and D A Gurnett (Department of Physics and Astronomy, University of Iowa, Iowa City, IA 52242; 319-335-1696)

C W Smith (Bartol Res. Inst., Newark, DE 19716)

During the Voyager 2 flyby of Uranus on 23-26 January 1986, strong electron plasma oscillations (Langmuir waves) were detected by the plasma wave instrument near 1.78 kHz prior to the inbound bow shock crossing. The Langmuir waves occurred in sporadic bursts for about one day until the spacecraft eventually crossed the bow shock at 0730 on 24 January 1986. The regions of space upstream of the shock can be divided into the undisturbed solar wind, the electron foreshock populated by energetic electrons, and the ion foreshock populated by energetic ions. The distance of the spacecraft upstream from the electron foreshock boundary can be calculated using the measured magnetic field and the spacecraft position together with a nominal shock model. This distance is called Diff. Using Langmuir wave bursts, changes in Diff, and the magnetic field direction, intervals have been identified when Voyager 2 was in the solar wind, electron foreshock, and the ion foreshock. These data are used to investigate the consistency of the standard model for Langmuir wave generation, as well as the implications of the observations for the position, shape, and motion of the bow shock.

SH41A-10 0830h POSTER

Plasma Wave Activity in the Deep Magnetosheath Inside the Far Flanks of the Earth's Bow Shock

S L Moses, E. W. Greenstadt, F. V. Coroniti, (TRW Space and Technology Group, One Space Park R1/2020, Redondo Beach CA 90278, 310-812-0075)

E. J. Smith (Jet Propulsion Laboratory, California Institute of Technology, 4800 Oak Grove Drive, Pasadena, CA 91109, 818-354-2248)

We present condensed, color spectrograms of plasma wave (pw) data, together with magnetic field records, collected during passes by ISEE 3 through the magnetosheath far downwind ($> 100 R_E$) from the Earth. The ISEE 3 trajectory and the spectrograms provide the first pw overviews of cross sections of the nightside magnetosheath both parallel and transverse to the tail axis. Magnetosheath plasma wave levels are intense, even though the plasma observed by the spacecraft may at times have flowed from the subsolar shock over 100 Earth radii forward from ISEE 3's position. Occasional interruptions of the pw activity may have been related to the geometry of the interplanetary magnetic field as convected to the spacecraft through the magnetosheath.

SH41A-11 0830h POSTER

Plasma Wave Activity Outside the Far Flanks of the Earth's Bow Shock

E. W. Greenstadt, S. L. Moses, F. V. Coroniti, (TRW Space and Technology Group, One Space Park R1/2020, Redondo Beach CA 90278, 310-812-0075)

E. J. Smith (Jet Propulsion Laboratory, California Institute of Technology, 4800 Oak Grove Drive, Pasadena, CA 91109, 818-354-2248)

We present ISEE-3 plasma wave (pw) and magnetic field data from traversals of the upstream region $100 R_E$ or so downwind from the subsolar bow shock. Upstream plasma wave activity is strongly controlled by the direction of the interplanetary magnetic field with the same sharp appearances and disappearances familiar in studies of ULF waves in the foreshock. Both involve backstreaming ion populations whose trajectories are governed by field connection and disconnection to some parts of the bow shock surface. While the upstream ULF turbulence is not as great as it is in front of the Earth, the plasma wave amplitudes are as intense as those seen near the shock subsolar point. The sensitivity of plasma wave detection gives pw signals a potential role in differentiating between passage of ULF growth regions and sudden immersions in fully developed foreshock activity.

SH41A-12 0830h POSTER

Evidence for the Parametric Decay of High Frequency ('1Hz') Whistler Waves in the Earth's Foreshock

A F Viñas

M. L. Goldstein (both at Laboratory for Extraterrestrial Physics, Code 692 NASA-Goddard Space Flight Center, Greenbelt, MD 20771; 301-286-6221 u2afv@lepacv.gsfc.nasa.gov; 301-286-7828, u2mlg@cdc910b2.gsfc.nasa.gov)

We have applied the theory of parametric instabilities recently presented by Viñas and Goldstein (1991a,b) to observations of high frequency magnetic fluctuations made by Hoppe et al. (1982). These observations show high frequency magnetic field fluctuations near the 1 Hz range of right hand polarized waves in the plasma frame propagating against the solar wind parallel to the mean magnetic field. The waves are convected by the solar wind so that they are observed by the spacecraft as left-hand polarized. In the solar wind frame, the fluctuations are circularly polarized in the plane perpendicular to the direction of propagation. Our analysis indicates that these fluctuations are unstable to the parametric decay instability. For this calculations we have extended the linear theory of parametric instabilities of a large amplitude, circularly polarized, dispersive wave for oblique propagation to the high frequency regime by including the electron inertia terms.

Hoppe, M. M., C. T. Russell, T. E. Eastman, and L. A. Frank. Characteristics of the ULF waves associated with upstream ion beams. *J. Geophys. Res.*, 87, 643, 1982.

Viñas, A. F. and M. L. Goldstein, Parametric instabilities of circularly polarized, large amplitude, dispersive Alfvén waves: excitation of parallel propagating electromagnetic daughter waves. *J. Plasma Phys.*, 46, 107, 1991a.

Viñas, A. F. and M. L. Goldstein, Parametric instabilities of circularly polarized, large amplitude, dispersive Alfvén waves: excitation of obliquely propagating daughter and sideband waves. *J. Plasma Phys.*, 46, 129, 1991b.

SH41A-13 0830h POSTER

Plasma Wave Dependence on the Shock Normal Angle in the Earth's Bow Shock

N Sckopke and R A Treumann (Max-Planck-Institut für extraterrestrische Physik, 8046 Garching, Germany)

The spectra of electric plasma waves in the vicinity of the Earth's Bow Shock wave have been investigated with emphasis on the dependence of their intensities on the shock normal angle θ_{BN} . It is found that the plasma wave intensity is a sensitive function of θ_{BN} . It is useful to distinguish between two different frequency bands, the upper containing the electron plasma waves, the lower the ion acoustic wave band. In quasi-perpendicular shocks the wave intensity in these two bands exhibits strong differences in dependence on the position of the satellite with respect to the shock and the foreshock region. A low frequency modulation of the plasma wave emissions is observed.

SH41A-14 0830h POSTER

Whistler Waves and Isotropization of Shock Electrons

D Krauss-Varban (ECE, University of California, San Diego, La Jolla, CA 92093, 619-534-8883)

Numerical tools such as the hybrid code have helped advance our understanding of the ion physics in collisionless shocks to a high level of sophistication in recent years. However, since such calculations do not resolve electron kinetic effects, there is considerable less theoretical insight concerning electron thermalization, heating, and acceleration. We have performed a series of test particle calculations of suprathermal electrons which move in hybrid-code generated fields of a quasi-perpendicular shock. The shock layer and downstream distribution functions are evaluated, and associated instabilities as well as non-adiabatic behaviour are discussed in the light of recent satellite observations. Such measurements indicate that the energetic electrons attain a nearly isotropic distribution by the time they reach the overshoot. In this work we concentrate on whistler waves that are thought to be excited by the anisotropy of the electrons as they enter the high magnetic field region. The generation of these waves as well as the ensuing pitch-angle scattering are studied using a full particle code. Our results indicate that the suprathermal electrons scatter in the whistler waves generated by the thermal (core) population, on a time scale much faster than the drift time through the shock. We propose that this mechanism is responsible for the observed near isotropy of the suprathermal electrons once they have reached the overshoot.

Plasma Wave Profiles of Earth's Bow Shock at Low Mach Numbers: ISEE 3 Observations on the Far Flank

E. W. GREENSTADT, F. V. CORONITI, AND S. L. MOSES

Electromagnetic Technology Department, TRW, Redondo Beach, California

E. J. SMITH

Jet Propulsion Laboratory, California Institute of Technology, Pasadena, California

The Earth's bow shock is weak along its distant flanks where the projected component of solar wind velocity normal to the hyperboloidal surface is only a fraction of the total free stream velocity, severely reducing the local Mach number. We present a survey of selected crossings far downstream from the subsolar shock, delineating the overall plasma wave (pw) behavior of a selected set of nearly perpendicular crossings and another set of limited Mach number but broad geometry; we include their immediate upstream regions. The result is a generalizable pw signature, or signatures, of low Mach number shocks and some likely implications of those signatures for the weak shock's plasma physical processes on the flank. We find the data consistent with the presence of ion beam interactions producing noise ahead of the shock in the ion acoustic frequency range. One subcritical case was found whose pw noise was presumably related to a reflected ion population just as in stronger events. The presence or absence, and the amplitudes, of pw activity are explainable by the presence or absence of a population of upstream ions controlled by the component of interplanetary magnetic field normal to the solar wind flow.

INTRODUCTION

The collisionless, high β (~ 1) shock in a magnetized plasma is in general a complicated phenomenon, but it should appear in its simplest manifestations when the Mach number is low. At its weakest, the shock has been assumed for years to display a smooth steplike jump or a dispersive wave profile, with modest jumps of magnetic field and density unlikely to disrupt the laminar flow of plasma from upstream to downstream states, while bestowing on it a mild temperature increase [Auer *et al.*, 1971; Mellott, 1985]. Relatively clean profiles of low- M shocks were in fact obtained analytically and experimentally two decades ago, but cases were necessarily simplified to achieve both analytic solutions and reproducible laboratory results [Tidman and Krall, 1971; Robson, 1969].

Satellite measurements in space plasmas offered the first opportunities to observe nature's solutions to the collisionless shock problem and to test the validity of theory- and laboratory-bound simplifications, but low- M shocks have turned out to be relatively scarce in the accessible extraterrestrial environment where most missions have gone. The Earth's bow shock is commonly strong ($M > 5$) in its subsolar region, where the great bulk of natural shock observations have been made, although solar wind variability has occasionally produced low- M conditions. Interplanetary shocks launched by solar activity or coronal inhomogeneities are often weak ($M \sim 2$), but they are encountered unsystematically and pass deep space probes too fast to reveal their structures to any but the fastest instruments and sampling systems. Nevertheless, interest in, and the importance of documenting, weak shocks has motivated investigators to collect and examine the available events, with somewhat surprising results: The presumably simplest (or borderline

simplest) of shock displays have included nonlaminar cases with unexpected heating [Thomsen *et al.*, 1985] and unanticipated magnetic and plasma wave profiles compatible with the presence upstream of small numbers of reflected ions not always detectable by particle instruments [Greenstadt and Mellott, 1987; Mellott and Greenstadt, 1988].

The chief indirect evidence for reflected ions has been the occurrence of elevated plasma wave (pw) signals between 10 Hz and 3 kHz, in the range of lower hybrid and ion acoustic frequencies in the otherwise undisturbed interplanetary magnetic field (IMF) immediately outside of low- M shock ramps. The signals are attributable to ion beam instability and are detectable because of the relatively high sensitivity of pw detectors to waves produced by even low densities of counter-streaming protons. The number of cases on which the pw evidence has been based has been small, however, but study has recently begun on a massive collection of weak shock observations made by ISEE 3 during its repeated crossing of the downwind bow shock in 1982 and 1983. The collection contains mostly low- M shocks because much of the satellite's time was spent where the weakened bow shock approaches its asymptotic Mach cone far downwind from Earth [Greenstadt *et al.*, 1990]. The purpose of this report is to confirm and enlarge the earlier results with a more comprehensive, although still preliminary survey of cases covering a range of local Mach numbers and IMF orientations, from quasi-perpendicular (Q_{\perp}) to quasi-parallel (Q_{\parallel}).

The sections immediately following describe our form of data presentation, scheme of case selection, and method of defining shock strength and then present our examples and discuss our interpretation of them.

DATA PRESENTATION

Shock Subsets

The pool of 110 shock crossings described by Greenstadt *et al.* [1990] has been augmented, with the help of J. T. Gosling

Copyright 1992 by the American Geophysical Union.

Paper number 91JA03049.
0148-0227/92/91JA-03049\$05.00

SM22A-5 1330h POSTER

Solar Wind and IMF Control of the Magnetopause in a Tsyanenko Model with Tail Warping

M. Peredo (Hughes STX Corporation, at NASA/GSFC)
N. A. Tsyanenko (St Petersburg State University, RUSSIA, and Laboratory for Extraterrestrial Physics, NASA/GSFC)
S. A. Curtis and D. P. Stern (Laboratory for Extraterrestrial Physics, NASA/GSFC)
M. V. Malkov (Polar Geophysical Institute, Apatity, RUSSIA)

A new family of Tsyanenko 87 models incorporating plasma sheet warping effects, and organized according to Solar Wind (SW) and Interplanetary Magnetic Field (IMF) conditions has been derived. The new models are based on the recently expanded IMP/HEOS/ISEE modeling database [Tsyanenko et al., Spring 92 AGU]. The IMP/HEOS database used to construct the original 87 models lacked sufficient SW and IMF correlative information to allow binning by those parameters. Tsyanenko and Malkov added ISEE observations, doubling the modeling database to ~60,000 magnetic field averages; more importantly nearly 85% of the ISEE averages are tagged with corresponding SW and IMF data. We have divided the complete IMP/HEOS/ISEE data set into four bins according to the north-south component of the IMF: strongly northward ($B_z > 4$ nT), weakly northward ($0 < B_z < 4$ nT), weakly southward (-4 nT $< B_z < 0$) and strongly southward ($B_z < -4$ nT); furthermore, we have also divided the data according to three ranges of the solar wind dynamic pressure: low ($0 < p_{sw} < 1.5$ nPa), medium ($1.5 < p_{sw} < 2.5$ nPa) and high ($p_{sw} > 2.5$ nPa). The "effective" magnetopause has been extrapolated from the models, and the resulting response to SW and IMF variation compared to that reported by Sibeck, et al (1991 and 1992). Quantitative comparisons between our magnetopause surfaces and Sibeck's model will be discussed. Anticipated use of the models as a calibration tool for global MHD models will also be addressed.

SM22A-6 1330h POSTER

Correlation of Magnetotail Pressures and Densities From Galileo Plasma Observations

W. R. Paterson and L. A. Frank (both at: Department of Physics and Astronomy, The University of Iowa, Iowa City, IA 52242; 319-335-1864)
M. G. Kivelson (Institute of Geophysics and Planetary Physics, UCLA, Los Angeles, CA 90024; 310-825-3435)

During the first Earth flyby the plasma instrumentation aboard Galileo detected a variety of magnetotail plasmas. Some of these plasmas fit recognized categories; for example magnetosheath, lobe, or plasma sheet. Others are not easily classified though our current analysis suggests that we have observed some localized phenomena which may include regions of nonadiabatic acceleration and possibly magnetic flux ropes. We find that a comparison of measured pressures (P) and number densities (n) provides some degree of organization for this diverse set of observations. If we plot $\log P$ versus $\log n$ there appear to be two generally different plasma populations. The colder plasmas which include the lobe and the magnetosheath exhibit $\log P = \gamma \log n$ with γ less than one. This result may be a consequence of pressure balance. The warmer plasmas, which include the plasma sheet, are found overall to have $\gamma \geq 1$ with good linear correlation. However, on short time scales (~20 minutes) we find that γ is characterized by considerable variability even within the plasma sheet. We summarize our current understanding of these results.

SM22A-7 1330h POSTER

Thin Current Sheets in the Deep Geomagnetic Tail

T. J. Pulkkinen (Finnish Meteorological Institute, SF-00101 Helsinki, Finland)
D. N. Baker (Laboratory for Extraterrestrial Physics, Code 690 NASA-Goddard Space Flight Center, Greenbelt, MD 20771; 301-286-8112; NSSDCA::BAKER)
J. T. Gosling (LANL, Los Alamos, NM 87545)
N. Murphy (JPL, Pasadena, CA 91109)
J. A. Slavin and C. J. Owen (NASA/GSFC, Code 696, Greenbelt, MD 20771)

Very thin current sheets with thickness of the order of the ion Larmor radius or less have frequently been observed in the near-Earth tail in association with substorm activity. During the growth phase close to the inner edge of the plasma sheet and in the expansive phase throughout the mid-tail region these thin sheets are thought to play a key role in the dynamical sequence constituting magnetospheric substorms. However, the strong gradients in the X-direction and the rapid temporal evolution of the current sheet configuration make a detailed study of the properties of such current sheets difficult. On the other hand, at large geocentric distances the magnetic field configuration becomes much more one-dimensional and, outside of periods of strong magnetic activity, may remain time stationary for relatively long periods. A thin current sheet characterized by rapid variations in the magnetic field polarity, plasma temperature, and pressure is frequently observed to persist in the region $X < -200 R_E$, which is usually identified to be beyond the distant neutral line. We have investigated 45 events in January-March 1983, where ISEE-3 was found to rapidly cross from one lobe to another in the deep tail region. The current sheet thicknesses were estimated using the high-energy ion data for approximately half of the events; the average thickness is $\sim 1.1 R_E$, ranging from $0.1 R_E$ to $3.0 R_E$. The reversal of both B_z and B_y components in association with some of the crossings is suggestive of current filamentation. These results will be compared and contrasted with the near-Earth current sheet observations during substorm periods.

SM22A-8 1330h POSTER

Nonlinear Analysis of the Cross-field Current Instability in the Earth's Neutral Sheet

P. H. Yoon (At: Institute for Physical Science and Technology, University of Maryland, College Park, MD 20742)

A. T. Y. Lui (At: The Johns Hopkins University Applied Physics Laboratory, Laurel, MD 20723)

The development of the cross-field current instability is investigated for condition of the Earth's neutral sheet just prior to current disruption. Numerical solution of the quasi-linear kinetic equations shows the wave growth reaching the nonlinear stage in less than one ion gyroperiod. The ion drift speed is found to be reduced by $\sim 15-28\%$ of its initial value, accompanied by non-adiabatic heating of ions and electrons mainly along the magnetic field. The resulting anomalous resistivity is estimated to be about 11 to 12 orders of magnitude above the classical Coulomb resistivity. It is also estimated that the plasma in the instability region is subjected to a substantial net force injecting it earthward for a typical amount of current reduction resulting from the instability growth.

SM22A-9 1330h POSTER

A 2-D Kinetic Model of the Plasma Sheet with Nonuniform Temperature

Vera Yaronina and J. R. Kan (Geophysical Institute, University of Alaska Fairbanks, Fairbanks, Alaska 99775)

A two-dimensional (2-D) kinetic model of a quasi-equilibrium plasma sheet is formulated based on an exact solution of the time-independent Vlasov-Maxwell equations. The nonuniform temperature distribution is achieved by assuming that the plasma sheet consists of two components of Maxwellian protons and two components of Maxwellian electrons, each at a constant but different temperature. The magnetic field is self-consistently calculated in the noon-midnight meridian plane under a prescribed boundary condition chosen to be Tsyanenko field along the Sun-Earth line. The calculated magnetic field is in good agreement with the Tsyanenko field model in the noon-midnight meridian plane. The temperature and plasma density calculated from the model are in good agreement with the satellite data on temperature and density measured in the equatorial plasma sheet.

SM22A-10 1330h POSTER

Determination of Magnetotail Domains Utilizing Only Magnetic Field Data

Robert E. Bell, Margaret G. Kivelson, Robert L. McPherron (Institute of Geophysics and Planetary Physics, Department of Earth and Space Science, University of California, Los Angeles, CA 90024-1567)

A study of data from the ISEE 2 spacecraft is presented to develop criteria for determining the boundary between the lobes and the plasma sheet when only the knowledge of the magnetic field and the spacecraft's position is available. A significant increase in the variance of the magnetic field component transverse to the background field is seen at the lobe-plasma-sheet crossings. Magnetic field criteria are developed to distinguish the lobe from the plasma sheet by using a set of established boundary crossings, as determined by plasma data. Several months of ISEE 2 data are used for a statistical comparison between these criteria and traditional methods which use plasma data. The results are encouraging and would allow us to significantly increase our data sets for lobe studies by including data from spacecraft not equipped with plasma instrumentation.

SM22A-11 1330h POSTER

Determination of Magnetotail Orientation Using Remote Sensing of the Plasma Sheet Boundary Layer with $E > 35$ keV Ions

C. J. Owen, J. A. Slavin (Code 696, NASA/Goddard Space Flight Center, Greenbelt, MD 20771)
I. G. Richardson (Code 661, NASA/Goddard Space Flight Center, Greenbelt, MD 20771)
N. Murphy (MS169-506, Jet Propulsion Lab., Pasadena, CA 91109)
R. J. Hynds (Space Physics Group, Imperial College, London, SW7 2BZ, United Kingdom) (Sponsor: AGU Member)

We use energetic ion data from the ISEE-3 Energetic Particle Anisotropy Spectrometer (EPAS) to determine the orientation of the deep tail plasma sheet each time the spacecraft moves between the lobe and the plasma sheet boundary layer. Analysis of the turn-on or turn-off times of 90° pitch angle energetic ions in

different particle telescope/look direction combinations allows the determination of speed of the boundary relative to the spacecraft, and the angle of inclination of the boundary relative to the ecliptic plane. Assuming that this angle is broadly representative of the degree of twisting exerted on the magnetotail by the IMF, we use a large number of such crossings to statistically study this phenomena. We attempt to determine how the degree of twisting is affected by such controlling factors as distance from the Earth, and different solar wind parameters.

SM22A-12 1330h POSTER

Magnetic Field and Current Structure of the Magnetotail at $X = -33R_E$

Z. Kazmaž and G. L. Siscoe (UCLA Dept. of Atmospheric Sciences, Los Angeles, CA 90024-1565; ph. 310-825-7407; fax. 310-206-5219); N. A. Tsyanenko and R. P. Lepp (NASA GODDARD Space Flight Center, Greenbelt, MD 20771)

We will present the magnetic field and current vector maps of the geomagnetic tail using 16 years of IMP-8 magnetic field measurements. Maps are produced for equinoxes and solstices separately. The magnetic field for equinoxes shows symmetry around the solar magnetospheric z-axis while solstices' magnetic field pattern is shifted in the positive z-direction in the center of the tail and in the negative z-direction on the flanks. This is the effect of the Earth's dipole tilt on the tail magnetic field structure as predicted. The effect is more pronounced in the current patterns than in the magnetic field pattern. In the equinoxes, current vectors flow in the middle of the tail from dawn to dusk, divert on the dusk flank, and return to the dawn flank over the tail boundary. However, the current vectors for the solstices, start below the GSM equatorial plane on the dawn flank, rise above it in the center and end up below it on the dusk flank. Thus, the pattern shows neutral sheet warping very nicely. Fairfield's displaced ellipse model is found to fit the data very well.

SM22A-13 1330h POSTER

Magnetotail Dynamics and Configuration in the Presence of IMF B_y

K. K. Khurana (Inst. of Geophysics and Planetary Physics, UCLA, Los Angeles, CA 90024)

Ever since Dungey [1961] recognized that the Earth's magnetosphere is 'open' in the presence of a southward interplanetary magnetic field, a steady stream of investigations has confirmed and extended the concept of a magnetospheric convection system driven by the solar wind. Other investigators [Russell, 1972; Maezawa, 1976] subsequently proposed models of high latitude reconnection in the presence of a northward IMF. However, when the IMF is predominantly in the GSM Y direction, the three dimensional convection in the ionosphere-magnetosphere system is not understood very well. In this work, we propose a model of magnetospheric convection in the presence of IMF B_y .

We first provide further evidence that IMF B_y 'penetrates' only those quadrants of the Earth's magnetotail in which the addition of the newly opened magnetic flux tubes occurs. The presence of B_y on the closed field lines (which is in the same direction as the IMF B_z) is also confirmed. Our model of magnetospheric convection involves dawn-dusk convective flows rather than a static magnetic configuration. In the presence of a southward-dusk oriented IMF, reconnection at the dayside magnetopause adds magnetic flux preferentially to the north-dawn and south-dusk quadrants. Convection driven by the cross-tail electric field and the pressure gradient force, relieves this asymmetric cross-tail pressure in the magnetotail. When this cross-tail convection is imposed on the plasma sheet, shear flows between the northern and southern halves of the plasma sheet result causing the field lines in the plasma sheet to bend producing a B_y in the same direction as the IMF B_y . The model is consistent with the two-cell ionospheric convection models constructed from electric field observations by Heppner and Maynard [1987]

SM22A-14 1330h POSTER

Plasma Waves in Distant Tail Slow Shocks

S. L. Moses, E. W. Greenstadt, F. V. Coroniti, (TRW Space and Technology Group, One Space Park R1/2020, Redondo Beach CA 90278, ph. 310-812-0075, fax: 310-813-3916); B. T. Tsurutani (Jet Propulsion Laboratory, California Institute of Technology, 4800 Oak Grove Drive, Pasadena, CA 91109, ph. 818-354-2248)

The ISEE 3 mission to the distant geomagnetic tail provided strong evidence that the plasma sheet was often bounded by standing, nearly switch-off slow shocks. The ISEE 3 TRW plasma wave detector found that the slow shock interaction region contained strong upstream plasma oscillations and a mid-frequency (100 - 300 Hz) narrowband emission just above the ion plasma frequency. Using the highest time resolution measurements of the electric field, we show that the mid-frequency emissions are highly impulsive, often exhibiting amplitude increases of greater than 100 in one half-second sampling interval. We also show that a previously unreported intermediate frequency mode occur well above the ion plasma frequency, and extending up to the

Observations of Plasma Waves in the Solar Wind Interaction Region of Comet Giacobini-Zinner at High Time Resolution

S. L. MOSES, F. V. CORONITI, AND E. W. GREENSTADT

TRW Space and Technology Group, Redondo Beach, California

B. T. TSURUTANI

Jet Propulsion Laboratory, California Institute of Technology, Los Angeles

High-time-resolution spectra of plasma wave emissions detected in the interaction region of comet Giacobini-Zinner with the solar wind reveal a wave phenomenology much more complicated than first reported. Spectra often exhibit three or more independent peaks, which become more prominent the deeper into the interaction region the spacecraft traversed. The main peaks correspond to whistler emissions below the electron cyclotron frequency, a midfrequency peak near the maximum Doppler shift frequency for waves with $k\lambda_D = 1$, a high-frequency peak above the Doppler shift maximum frequency, and electron plasma oscillations at the plasma frequency. Similar multi-peaked spectra are also observed downstream from weak shocks at Earth, which suggests that the plasma wave generation mechanisms responsible need not require particle populations created by photoionization.

INTRODUCTION

One of the most prominent issues to arise after the encounter of the International Cometary Explorer (ICE) with comet Giacobini-Zinner on September 11, 1985, is whether the interaction of the solar wind with the heavy ions produced near the comet creates a bow shock around the comet. Measurements made by the ICE plasma wave detector (PWS) were among the data used to support the existence of a shock [Scarf *et al.*, 1986; Kennel *et al.*, 1986], and an analysis utilizing the Rankine-Hugoniot relations suggested that a low Mach number shock was crossed both inbound and outbound [Smith *et al.*, 1986]. These studies employed long time scale averages of the data to obtain a global picture of the comet encounter. In contrast, using numerical simulations of the ion pickup region, Omid *and Winske* [1988] argued that the solar wind did not encounter a single shock but was slowed by the cumulative effect of steepened magnetosonic waves, known as "shocklets", which increase in number and amplitude nearer the comet. This model is consistent with the signature of steepened magnetosonic waves in the magnetic field deep inside the interaction region [Tsurutani *and Smith*, 1986], the absence of a single identifiable shock transition, and electron plasma data in which shock-heated downstream plasma was interspersed with seemingly unshocked solar wind [Thomsen *et al.*, 1986]. However, it has not yet been shown that the steepened magnetosonic waves in the comet are causing the deceleration of the solar wind.

Similar magnetic field and plasma wave conditions were found at comet Halley during the encounters by the Giotto and VEGA spacecraft, and Tsurutani [1991] presents a detailed review of the phenomenology found at both comets. The magnetosonic waves detected upstream of Halley were reported to be of smaller amplitude, but more turbulent appearance, than those found at Giacobini-Zinner [Johnstone *et al.*, 1986] and it

has been suggested that this might be due to the greater distances over which waves were generated at Halley, which would allow more wave-wave interactions to occur. In general, the clean progression in the development of steepened magnetosonic waves observed at Giacobini-Zinner was not seen at Halley. Intense plasma wave activity was also observed at Halley, although the sensitivity of the plasma wave detectors flown on those spacecraft was at least an order of magnitude poorer than for the ICE PWS (this is due to the extremely long length, 90 m tip to tip, of the ICE electric field antennas).

The purpose of this paper is to present the plasma wave observations made at Giacobini-Zinner on a time scale that resolves individual steepened magnetosonic waves and compare them with similar high-resolution observations of weak terrestrial bow shocks. On this scale the wave spectra at the comet are highly variable and reveal more wave modes than previously assumed, but similarities can still be found between the cometary spectra and those from weak shocks at Earth. In the next section we will illustrate the evolution of the wave spectrum as the magnetosonic waves steepen and describe the different wave modes. The third section presents the plasma wave data from weak quasi-parallel shocks observed on the flanks of the Earth's bow shock and contrasts them with the comet examples. The fourth section contains a discussion of the results in the light of previous wave generation models. This is followed by a brief summary.

GIACOBINI-ZINNER OBSERVATIONS

Figure 1 shows the magnetic field data for the 1-hour interval containing the inbound shock crossing (top panel) and 5-min-averaged electric field spectra which illustrate the shocklike characteristics of the plasma waves as used by Kennel *et al.* [1986] in the initial report on plasma waves in the solar wind interaction region. The upstream region was found to contain electron plasma oscillations at the plasma frequency, f_p , and broadband emissions with frequencies from about 100 Hz to nearly 10 kHz. These signals are similar to waves observed in the ion foreshock at Earth and are often called (for lack of a

Copyright 1992 by the American Geophysical Union.

Paper number 92JA01601.

0148-0227/92/92JA-01601\$05.00

dependent upon the upstream beta and the upstream Mach number and is highly correlated with the ratio of criticality, an upstream parameter which encompasses both the plasma beta and the Mach number. Thus, we find that the ratio of criticality and the solar wind helium content are the two important parameters in determining whether ion cyclotron or mirror mode waves will dominate the magnetosheath wave activity.

SM22A-20 1330h POSTER
CORRELATED OBSERVATIONS OF WAVES AND IONS IN THE EARTH'S MAGNETOSHEATH

L.A. Lockband, (Astronomy Unit, Queen Mary and Westfield College, Mile End Road, London E1 4NS; tel. +44 (71) 975 5555; fax. +44 (81) 981 9587); A. Fazakerley, A. Coates, (Mullard Space Science Laboratory, University College London, Holmbury St. Mary, Surrey RH5 6NT, UK; tel. +44 (483) 274111); D. Burgess, S. Schwartz (Astronomy Unit, Queen Mary and Westfield College, Mile End Road, London E1 4NS; tel. +44 (71) 975 5555; fax. +44 (81) 981 9587); M. Dunlop (Dept. of Physics, Imperial College of Science, Technology and Medicine, London, UK)

We report on correlated observations of waves and ion distributions in the Earth's magnetosheath region. We have selected 6 periods from when the AMPTE-UKS magnetometer and ion instruments gathered data for the entire magnetosheath from the bow shock to the magnetopause. Time series of various transport ratios such as the Alfvén ratio, compressibility, and parallel compressibility are analysed in conjunction with the standard quantities (such as the temperature anisotropy ratio) to identify periods when various wave phenomena may be expected to occur. This approach has been motivated by recent theoretical work and simulations where it is argued that the dominance of either the mirror or ion cyclotron instability will be most apparent in the transport ratios. We compare the occurrence of different wave types with instability criteria derived from both MHD and kinetic theory. We also report on a study of the effects of these instabilities on the ion distribution functions.

SM22A-22 1330h POSTER
Effects on Thermal Ions, H⁺, He⁺ and O⁺ Associated with Ion Cyclotron Waves

S Geyer, E.J. Anderson (Both at: Johns Hopkins University Applied Physics Laboratory, Laurel MD 20723; 301-943-5000; SPAN: AMPTE:ANDERSON)
S A Fuselier (Lockheed Palo Alto Research Laboratory, Palo Alto CA, 94304)

Electromagnetic ion cyclotron waves are widely thought to interact with ions heavier than protons and some evidence has shown heating effects and phase bunched interactions. Increased He⁺ densities have also been attributed a causative role in enhancing amplification of waves with equatorial frequencies higher than f_{He^+} . We examine distributions of H⁺, He⁺ and O⁺ over energies from the spacecraft potential to 17 keV using the HPCCE instrument on AMPTE/CCE. In this study we concentrate on the low energy, < 500 eV, populations. A total of 49 intervals were chosen on the basis of EMIC wave activity: 24 for which EMIC waves were prevalent, and 25 in which no EMIC waves were observed on the orbit. We find a distinction between events occurring near, ± 3 hours, of noon, and those occurring near dawn MLT. For events on the dayside there is a one to one correlation between EMIC waves and heavy ion distributions exhibiting perpendicular heating; without EMIC waves exhibit $T_{\perp} > T_{\parallel}$ whereas intervals with EMIC waves uniformly have $T_{\perp} < T_{\parallel}$. For dawn events, the plasma has a plasma sheet like keV electron population, and measurable He⁺. The ion distributions for the dawn events are generally field aligned, $T_{\perp} > T_{\parallel}$, regardless of whether EMIC waves are observed. For the dayside events, the heavy ion concentration shows a positive correlation with EMIC waves, but detailed examination of the lowest energies, < 10 eV, shows no correlation in heavy ion concentration with the waves. The enhanced heavy ion densities above 50 eV is attributable to the perpendicular heating of the ions.

SM22A-23 1330h POSTER
Magnetic Field Direction Control of Plasma Wave Emissions in the Earth's Magnetosheath

S.L. Moses, F.V. Coroniti, E.W. Greenstadt (TRW Space and Electronics Group, One Space Park, R12144, Redondo Beach CA 90278)

Prior to the ISEE-3 encounter with Comet Giacobini-Zinner the spacecraft performed several passes through the far downstream magnetosheath. The magnetosheath often contains intense broadband electrostatic plasma wave emissions—the so-called ion acoustic waves—in the frequency band between the ion and electron plasma frequencies. The ISEE-3 data shows that the wave amplitudes are controlled by the direction of the magnetic field in the sheath, with wave emissions disappearing when the field is perpendicular to the flow direction. This effect is independent of the direction of the field in the plane perpendicular to the flow and does not correlate with magnetic connection to the magnetopause. The correlation with field direction is less apparent at higher time resolution, although the wave dropouts sometimes correspond with decreases in the magnetic field magnitude. These results are the first indication of magnetic field direction influencing the appearance of downstream electrostatic waves.

SM22B CA: 415 Tues 1330h
Magnetic Reconnection: Onset of Magnetospheric Substorms and Solar Eruptive Processes II (joint with SH)
Presiding: B Sonnerup, Dartmouth College

SM22B-1 1330h INVITED
Observational Aspects of Magnetic Reconnection at Earth's Magnetopause

J.T. Gosling (MS D466, Los Alamos National Laboratory, Los Alamos, NM 87545; 505-667-5389; jgosing@lanl.gov)

Measurements made in the vicinity of the magnetopause have provided a direct demonstration that reconnection between the interplanetary magnetic field (IMF) and the Earth's magnetic field commonly occurs. These measurements tell us much about where and when reconnection occurs as well as about the structure of the layer of reconnected field lines at the magnetopause, but tell us very little about details of the actual reconnection process itself within the so-called "diffusion region". Direct evidence for reconnection at the magnetopause can be found in observations of bulk plasma accelerations and plasma reflections and transmissions that occur there, in offsets between the ion and electron edges of the low latitude boundary field (LLBL), and in systematic oscillations in the normal magnetic field component popularly known as flux transfer events. Interestingly, reconnection at the magnetopause does not appear to lead directly to either substantial plasma heating (although some occurs) or particle acceleration. Slow shocks seem to be extremely rare within the layer of reconnected field lines at the magnetopause. Reconnection appears to occur in both a quasi-stationary mode and in a time-dependent mode. It occurs commonly in the subsolar regions of the magnetopause for a wide range of local field shears, and at high latitudes and along the flanks of the magnetosphere when the external and internal magnetic fields are nearly antiparallel. Reconnection has been observed between the IMF and both the closed magnetospheric field lines at low latitudes and the "open" field lines of the polar caps and tail lobes. At times, reconnection is entirely responsible for the formation of the LLBL, as well as the plasma mantle. The observations suggest that, in addition to large magnetic shear, the reconnection process favors intervals of low plasma beta in the magnetosheath.

SM22B-2 1355h
Possible Conjugate Reconnection at the High-Latitude Magnetopause

W.C. Feldman, B.L. Barraclough, R.D. Belian, T.E. Cayton, E.W. Hones, P. Lee (Mail Stop D466, Los Alamos National Laboratory, Los Alamos, NM 87545; 505-667-7372; e-mail wfeldman@ssscx1.lanl.gov).

R.P. Lepping, J.I. Trombka, R. Starr (Code 691, NASA/Goddard Space Flight Center, Greenbelt, MD 20771), **J. Moersch and S.W. Squyres** (Cornell U., Space Sciences Building, Ithaca NY 14853)

Coordinated analysis of data sets from X-ray, energetic electron, Interplanetary Magnetic Field (IMF), and solar wind plasma experiments yields a comprehensive picture of the simulated precipitation of trapped relativistic electrons simultaneously onto both high-latitude polar caps in response to a substorm initiated at about noon U.T. on 17 Dec. 1992. As detected in hard X rays by a long-duration Antarctic balloon-borne sensor, precipitation began at 13:30 U.T., just 15 minutes after an abrupt northward turning of the IMF at IMP 8. This occurrence triggered the recovery phase of the substorm. Whereas 50-100 keV electrons were injected at synchronous orbit at substorm onset (about 12:20 U.T.), higher energy electrons (100-200 keV) did not begin increasing there until between 13:30 and 13:45 U.T. The sharp enhancement of hard X rays terminated at 15:20 U.T., about 20 minutes after the IMF turned abruptly southward at IMP 8. Precipitating electrons having energies in the range between 0.25 and 1 MeV were detected above both north and south polar caps during this two-hour period. These observations are readily explained by, and strongly suggest the occurrence of, conjugate magnetic reconnection tailward of both geomagnetic cusps.

SM22B-3 1410h INVITED
The Status of the Collisionless Ion Tearing Instability as a Trigger for Magnetospheric Substorms

E.L. Pritchett (Department of Physics, UCLA, Los Angeles, CA 90024-1547)

The relation of reconnection in the geomagnetic tail to the spontaneous collisionless tearing mode has had a long and tortured history. On numerous occasions the hopes of tearing aficionados have been dashed by new observational and theoretical discoveries, only to be resurrected in a modified form at a later date. We review the key stages in this history: the proposal of the electron tearing mode, the demise of electron tearing due to the discovery of the average normal magnetic field component (B_z) in the plasma sheet, the proposal of the ion tearing mode, the stabilizing effects of adiabatic electron motion, attempts to remove electron stabilization by pitch-angle scattering resulting from either wave turbulence or chaoticization of electron orbits, ion tearing in thin current sheets, and finally the conclusive (?) evidence from theory and simulations indicating that electron compressibility leaves no parameter space for a spontaneous ion tearing mode in the near-Earth plasma sheet.

SM22B-4 1435h
Onset and Growth of Collisionless Magnetic Reconnection in Sheared Field Reversals

M. Kuznetsova (Space Research Institute, R-117810 Moscow, Russia) **J. Buchner** (Max Planck Institut Extraterrestrische Physik, Berlin D-12489; tel. fax: (04930) 6392 3937; INTERNET: jbaTmpe.wza-berlin.de); **L.M. Zelenyi** (Space Research Institute, R-117810 Moscow, Russia)

Plasma parameters both in the Solar corona and in the Earth magnetospheric tail imply that collisionless plasma mechanisms should cause the observed current sheet disruptions. Solar and magnetotail current sheets related to these disruptions are, in general, embedded in curved and sheared magnetic fields. Recently we have analysed the conditions of destabilization of a collisionless current sheet in the presence of magnetic shear. We obtained thresholds beyond which the onset of spontaneous collisionless ion tearing mode instability should take place (Buchner et al., 1991).

Here we present the results of an extended analysis of the kinetic stability theory of a current sheet in a curved and sheared magnetic field reversal with respect to a tearing mode perturbation. In our analysis we newly take into account the coupling between quasi-parallel (electric field perturbation directed parallel to the ambient magnetic field) and quasi-perpendicular mode components.

We obtain that, in contrast to the results of Wang et al. (1990), an unstable branch of tearing mode instability with a growth rate less than the electron bounce frequency can be excited. The dependencies of the growth rate of this instability on the shear- and normal-field components as far as on the wave length of the mode have been obtained. The resulting tearing mode destabilization takes place favourably for an inclination of the magnetic field near the quasi-neutral plane at about 45 degrees with respect to the neutral plane and for values of B_z of the order of B_s , both exceeding one tenth of the asymptotic magnetic field strength. Our theory reveals that in this situation a collisionless ion tearing mode can be triggered and magnetic flux ropes are formed. The growth of the unstable tearing mode is shown to be accompanied by the generation of magnetic field aligned electric fields and ion acceleration.

J. Buchner et al., *Geophys. Res. Lett.*, 18, No. 3, 385, 1991.
X. Wang et al., *J. Geophys. Res.*, 95, No. 9, 15,047, 1990.

SM22B-5 1450h
Transition to Whistler Mediated Magnetic Reconnection

M.E. Mandt and J.E. Drake (Both at: Institute for Physical Science and Technology, University of Maryland, College Park, MD 20742; ph. 301-405-1495; fax 301-405-1678; Internet: mem@uap.umd.edu); **R.E. Denton** (Dept. of Physics and Astronomy, Dartmouth College, Hanover, NH 03755) (AGU Sponsor: M.E. Mandt)

The transition in the magnetic reconnection rate from the resistive magnetohydrodynamic (MHD) regime where the Alfvén wave controls reconnection to a regime in which the ions become unmagnetized and the whistler wave mediates reconnection is explored with 2-D hybrid simulations. In the whistler regime the electrons carry the currents while the ions merely provide a neutralizing background. Results will be presented in which the electrons have zero and finite inertia. A simple physical picture is presented which illustrates the role of the whistler in driving reconnection and the rate of whistler mediated reconnection is calculated analytically. The development of an out-of-plane component of the magnetic field is an observable signature of whistler driven reconnection. Whistler driven reconnection has been observed in laboratory experiments.

SM22B-6 1505h
Hybrid Modeling of Collisionless Magnetic Reconnection: Result

M. Hesse (Code 696, NASA/Goddard Space Flight Center, Greenbelt, MD 20771)
D. Winske (Los Alamos National Laboratory, X-1, MS F645, Los Alamos, New Mexico 87545)

While it is commonly accepted that magnetic reconnection plays an important role in space plasmas, the microphysical nature of reconnection is still subject of current discussion. One of the debated mechanism is entirely collisionless, based on the Landau resonance of current carrying ions. Recent results of our 2 1/2 dimensional hybrid model of this type of magnetic reconnection will be presented. The role of scaling parameters, such as electron/ion temperature ratio, current sheet thickness, and the dependence of the reconnection mechanism on isotropizing fluctuations will be discussed. Furthermore, we will show signatures of reconnection in the magnetic field, and in the ion and electron flows and distribution functions, such as could be found in satellite based observations. We will also discuss reconnection in current sheets with magnetic normal components.

SM22B-7 1550h INVITED
Tailward Streaming Magnetic Structures in the Distant Tail

A. Nishida (ISAS, 3-1-1 Yoshinodai, Sagami-hara 229, Japan; fax 81 427 59 4236; Internet: nishida@tdl.isas.ac.jp)

Since the launch in July, 1992, Geotail has been conducting fruitful mission in the distant tail beyond the lunar distance. This paper summarizes the observations of the tailward convecting magnetic structures in the distant tail and discusses their relation to magnetic reconnection.

It is confirmed that the plasmoid characterized by a bipolar structure in Bz

S
M

ORIGINAL PAGE IS OF POOR QUALITY

This page may be freely copied.

PRECEDING PAGE BLANK NOT FILMED

first-order Fermi or diffusive shock acceleration is irrelevant. It is found that the reflected ions from the shock front releases their free energy of the ring distribution in the velocity space into the downstream electrons, and that the nonthermal, power law-like spectrum of the electron can be formed when the upstream plasma velocity $\gamma v/c$ exceeds about unity, where γ is the Lorentz factor of the upstream flow. The downstream energy spectrum, however, remains in the thermal, Maxwellian when the upstream plasma velocity $\gamma v/c < 1$. Two processes are important for the nonthermal particle acceleration: one is the relativistic cyclotron resonance between electrons and the magnetosonic waves excited by the gyrating reflected ions. Since the high frequency magnetosonic waves are almost linearly polarized, the electrons can resonate with the waves. Another process is the ExB drift acceleration by the wavelets of nonlinear steepened magnetosonic waves. The wavelets can tend to diffuse particles within the velocity space.

SH42D-11 1630h

Left-Hand Polarized Magnetic Waves at Whistler Mode Frequencies

H.K. Wong (Department of Space Sciences, Southwest Research Institute, San Antonio, TX 78228-0510; 210-522-3627; SPAN: SWRI:KIT)

C.W. Smith (Bartol Research Institute, University of Delaware, Newark, DE 19716; 302-831-8114; SPAN:BARTOL:UDBRI:CHUCK)

It is shown that an anisotropic electron beam is capable of generating both left and right hand parallel propagating electromagnetic waves with frequencies at the whistler mode range. The crucial parameters that determine the instability are the temperature anisotropy, beam density, and the ratio of the beam temperature and the temperature of the background plasma. For the physical parameters under consideration, the left-hand wave typically has higher growth rate than the right-hand wave. The free energy source of this instability is the temperature anisotropy but the beam speed can significantly alter the wave frequency. Numerical and analytical calculations will be presented to demonstrate the conditions under which the instability can occur and the possible applications of this instability to whistler waves observed in planetary bow shocks will be discussed.

SH42D-12 1645h

Whistler Waves Upstream of Neptune's Bow Shock

Charles W. Smith (Bartol Research Institute, University of Delaware, Newark, Delaware 19716),

Hung K. Wong (Southwest Research Institute, San Antonio, Texas 78284), Melvyn L. Goldstein (NASA/GSFC, Code 692, Greenbelt, Maryland 20771), and Barry H. Mauk (JHU/APL, Johns Hopkins Road, Laurel, Maryland 20723).

We have examined Voyager 2 magnetometer measurements recorded upstream of Neptune's bow shock in a search for whistler wave activity arising from any of several possible sources. Part of the motivation for this study is the reported observation of unusually intense whistler mode activity upstream of the Uranian shock¹ arising from gyrating proton populations and the excitation of multiple whistler mode waves by energetic electrons². A recent instability analysis³ has shown that the simultaneous excitation of multiple whistler mode waves is possible over a wider range of plasma and beam parameters than were inferred to exist at Uranus while the excitation of left-hand polarized waves at similar wave frequencies is also possible⁴. We have sought evidence of the above instability mechanisms upstream of Neptune's bow shock as well as instances of more familiar whistler mode forms. We report on the results of this search and offer a general survey of the magnetic waves in Neptune's foreshock⁵.

- 1) Smith, C.W., M.L. Goldstein, and H.K. Wong, *J. Geophys. Res.*, **94**, 17,035-17,048, 1989.
- 2) Smith, C.W., H.K. Wong, and M.L. Goldstein, *J. Geophys. Res.*, **96**, 15,841-15,852, 1991.
- 3) Wong, H.K., and C.W. Smith, *J. Geophys. Res.*, submitted, 1993.
- 4) Wong, H.K., and C.W. Smith, *Geophys. Res. Lett.*, submitted, 1993.
- 5) This work was supported by NASA grant NAGW-3445 and Jet Propulsion Laboratory contract #959167 to the BRI.

SH42D-13 1700h

Linear Damping of Wideband Upstream Whistlers

C.T. Russell, D.S. Orlovski, and G. Le (All at: Institute of Geophysics and Planetary Physics, University of California, Los Angeles, CA 90024-1567; tel. 310-825-3188; email ctrussell@igpp.ucla.edu)
D. Krauss-Varban and N. Omidi (Department of Electrical and Computer Engineering and California Space Institute, University of California, San Diego, La Jolla, CA)
M.F. Thomsen (Los Alamos National Laboratory, Los Alamos, NM)

Previous studies of upstream whistlers at Venus by Orlovski et al. [1993] suggested that damping rates strongly depend on properties of the solar wind electrons, such as temperature anisotropy and relative core/halo density ratio. Detailed analysis of the Doppler-shift and the whistler dispersion relation indicated that upstream whistlers propagate obliquely in a wide band (10-100 times the proton gyrofrequency) in the plasma frame. In this paper we present results of calculations of damping lengths of wideband whistlers using the sum of 7 drifting bi-Maxwellian electron distributions as a best fit to the ISEE 1 electron data. For 3 cases, when upstream whistlers are observed, convective damping lengths derived from the two spacecraft are compared with theoretical results. We find that the calculated convective damping lengths vary from about 200 to 2000 km consistent with the observations. We also show that the slope of plasma frame spectra of upstream whistlers, obtained by direct fitting or by "inverse" phase shifting of the observed spectra, is between 3.5 and 4.5. The spectral characteristics, proximity to the shock as well as propagation and damping properties indicate that these waves cannot be generated in the solar wind. Instead the observed upstream whistlers in the shock foot and/or ramp must grow by a variety of cross-field drift electron instabilities. Finally we find that in all 3 cases the upstream plasma was stable over the frequency range of the observed waves. In fact the waves were strongly damped.

SH51A CA: Arena Fri 0830h
Collisionless Shock Physics II Posters
Presiding: M Shea, Phillips Lab

SH51A-1 0830h POSTER

Investigation of Bow Shock in a Laboratory Simulated Earth's Magnetosphere

Gung Yur and H.U. Rahman (Both at: Institute of Geophysics and Planetary Physics, Univ. of California, Riverside, California 92521; 909-787-4510/909-787-4588)
Joachim Birn (Los Alamos National Laboratory, SST-8, MS D438, Los Alamos, New Mexico 87545; 505-667-9232)

Solar wind interaction with the Earth's magnetic field is studied in a laboratory simulated magnetosphere by interacting a flowing magnetized plasma with a stationary dipole field. Particular emphasis is placed on the investigation of the formation of bow shock and its dependence on the polarity of the IMF. The bow shock is identified by using a gated optical imager (GOI) and detailed measurements obtained by using two-dimensional magnetic probes, double Langmuir probe and double-sided Faraday cups. The GOI is capable of imaging the model magnetosphere for less than 1 μ sec gate width compared to the 100 μ sec duration of plasma interaction. A series of photographs will be presented that will show the dynamic behavior of the interaction and the formation of the bow shock. When the Alfvén mach number is larger than unity, a bow shock appears in front of the simulated magnetosphere. These photographic images for different orientations of the IMF. The measurements of the magnetic field, plasma parameters and the current density are presently underway. These measurements will provide quantitative and detailed information about shocked and unshocked regions and the type of the bow shock that forms in the laboratory simulated magnetosphere.

*Research supported by NSF and IGPP/LANL.

SH51A-2 0830h POSTER

3D Proton Velocity Near Mars

E. Kallio, H. Koskinen (Finnish Meteorological Institute, Department of Geophysics, P.O. Box 503, SF-00101, Helsinki, Finland, Internet: Esa.Kallio@fmi.fi); S. Barabash, R. Lundin, O. Norberg (Swedish Institute of Space Physics, Kiruna, Sweden); J.G. Luhmann (Institute of Geophysics and Planetary Physics, University of California, Los Angeles)

The proton velocity measurements made by ASPERA plasma composition instrument onboard the Phobos-2 spacecraft in early 1989 are analysed. Characteristics of the solar wind deflection around Mars are studied by calculating three dimensional (3D) velocity distribution of proton plasma downstream of the Martian bow shock. Deflection of the proton flow near the bow shock and almost stopping at the magnetopause were observed.

Occasionally, a rather smooth transition layer between the magnetosheath plasma and the magnetospheric plasma were detected. When the velocity profiles were compared with a gas dynamic model, the location of the observed boundaries as well as the general behaviour of the flow were found to be rather well described by the model. However, the observed differences between the data and the model suggest that non-single-fluid phenomena, probably associated with pick-up and kinetic processes, also affect the interaction process.

SH51A-3 0830h POSTER

Pioneer Venus Orbiter Retarding Potential Analyzer Observations of the Electron Component of the Solar Wind and Observations of Venus Bow Shock Crossings and the Magnetosheath Region.

D. Gifford, D.E. Jones, and N. Yamaguchi (All from: Department of Physics and Astronomy, Brigham Young University, Provo, UT, 84602; 801-378-2108)
W. C. Knudsen (Knudsen Geophysical Research, 18475 Twin Creeks Rd., Monte Sereno, CA 95030)
J. D. Mihalov (NASA-Ames Research Center, Moffett Field CA, 94035-1000)

Using an improved expression for the grid potential distribution for the Retarding Potential Analyzer, a comparison of the suprathermal electrons measured by this instrument with the Plasma Analyzer proton densities when Pioneer Venus Orbiter was beyond the ionopause and outside the ionotail of Venus suggest that when observations in which solar EUV produced electrons from the ORPA are deleted, the densities measured by these two instruments track very well. It is therefore possible to utilize the ORPA suprathermal electron observations to infer the solar wind electron densities, thereby enhancing our ability to conduct high (seconds) time resolution studies of Venus bow shocks. An extensive analysis program using the ORPA suprathermal electron observations to study a number of Venus bow shock crossings and the electron density and temperature distribution in the region between the bow shock and the ionopause under varying solar conditions is presently underway. Some preliminary results of this study will be presented.

SH51A-4 0830h POSTER

Electron Plasma Oscillations in the Foreshock: Comparison of Occurrence at PVO and ISEE 3

E.W. Greenstadt, S.L. Moses, F.V. Coroniti (TRW, RI-2144, One Space Park, Redondo Beach, CA 90278); G.K. Crawford, R.J. Strangeway (Inst. Geophys. and Planet. Phys., University of California, Los Angeles, CA, 90024-1567)

Crawford et al. [1993] recently implemented a program to map the occurrence of plasma wave emissions in normalized coordinates in the Venus foreshock. We will present here preliminary results of applying this program to data from ISEE 3 traversals of the Earth's foreshock. The ISEE 3 trajectory during the heliocentric orbit insertion phase carried it through regions of the foreshock not normally encountered by Earth-orbiting spacecraft. Results show that the program organizes the ISEE 3 data illustrating the control of wave occurrence by magnetic field geometry. We will present a comparison of the terrestrial foreshock boundary provided by this mapping with the earlier results from Venus.

SH51A-5 0830h POSTER

Suprathermal He²⁺ and the Origin of Energetic Ions in the Earth's Foreshock Region

S.A. Fuselier, (Lockheed Palo Alto Research Laboratory, Palo Alto, California 94304; (415) 424-3334; LOCKBD:FUSELIER)

M.F. Thomsen, (Los Alamos National Laboratory, Los Alamos, NM, 87545)
F.M. Ipavich, (University of Maryland, College Park, MD, 20742)

Energetic ion distributions (with energies of a few keV extending to over 100 keV/e, also called diffuse ion distributions) upstream from the Earth's quasi-parallel bow shock have approximately solar wind composition (i.e., ~4% He²⁺). In contrast, field-aligned ion beams observed in the foreshock region upstream from the Earth's bow shock have He²⁺ concentrations that average two orders of magnitude below that in the solar wind. Thus, while it is clear that field-aligned beams are not the major source of energetic ions in the foreshock region, the seed population (i.e., the suprathermal stage through which the solar wind source particles pass in the acceleration process) for these ions has not been identified. We report He²⁺ and He³⁺ observations from the ISEE-1 and -2 spacecraft which suggest

Plasma Waves Downstream of Weak Collisionless Shocks

F. V. CORONITI, E. W. GREENSTADT, AND S. L. MOSES

TRW Space and Electronics Group, Redondo Beach, California

E. J. SMITH AND B. T. TSURUTANI

Jet Propulsion Laboratory, California Institute of Technology, Pasadena

In September 1983 the ISEE 3/ICE spacecraft made a long traversal of the distant dawnside flank region of the Earth's magnetosphere and had many encounters with the low Mach number bow shock. These weak shocks excite plasma wave electric field turbulence with amplitudes comparable to those detected in the much stronger bow shock near the nose region. Downstream of quasi-perpendicular (quasi-parallel) shocks, the E field spectra exhibit a strong peak (plateau) at midfrequencies (1–3 kHz); the plateau shape is produced by a low-frequency (100–300 Hz) emission which is more intense behind quasi-parallel shocks. Polarization measurements made in the very steady magnetic field conditions downstream of two quasi-perpendicular shocks show that the low frequency signals are polarized parallel to the magnetic field, whereas the midfrequency emissions are unpolarized or only weakly polarized. A new high frequency (10–30 kHz) emission which is above the maximum Doppler shift frequency is clearly identified as a separate wave component. High time resolution spectra often exhibit a distinct peak at high frequencies; this peak is often blurred by the large amplitude fluctuations of the midfrequency waves. The high-frequency component is strongly polarized along the magnetic field and varies independently of the lower-frequency waves.

1. INTRODUCTION

From September through December of 1983 the ISEE 3 spacecraft traversed the far dawnside region of the magnetosheath and had multiple encounters with the bow shock [Greenstadt *et al.*, 1990]. Since the shock normal is nearly orthogonal to the solar wind flow direction, the far flank shocks have low Alfvén and magnetosonic Mach numbers. Thus the ISEE 3 data set provides a unique opportunity to investigate the plasma, magnetic field, and plasma wave properties of collisionless shocks in a Mach number regime which has rarely been accessible to previous satellite studies. In this paper we focus on plasma wave electric field measurements in the region immediately downstream of several typical quasi-parallel and quasi-perpendicular flank shocks. Strong shocks in the nose region of the magnetosheath [Rodriguez and Gurnett, 1975] and interplanetary shocks [Kennel *et al.*, 1982] generate intense electric field turbulence in the downstream region. The weak flank shocks might be expected to stimulate a significantly lower level of downstream wave noise. We find, however, that the electric field spectral amplitudes and spectral shapes detected behind the flank shocks are quite comparable to the wave properties observed behind the nose region shocks.

In the subsolar region of the Earth's bow shock, Rodriguez [1979] identified three types of electrostatic plasma waves which occurred in the magnetosheath: (1) a low-frequency component with a peak near 100–300 Hz, well below the ion plasma frequency ($2\pi f_{pi} = (4\pi ne^2/m_i)^{1/2}$) and with a smoothly falling spectrum above the peak frequency; (2) an intermediate-frequency component with frequencies between the ion and electron plasma frequencies ($f_{pi} < f < f_{pe}$) and a peak near 1 kHz; and (3) a high-

frequency component at the electron plasma frequency. The low-frequency component resembles the wave spectra typically observed within the shock front [Rodriguez and Gurnett, 1975; Gurnett, 1985], whereas the intermediate- and high-frequency components had spectra which are similar to wave emissions in the upstream region. Rodriguez [1979] suggested that the intermediate-frequency waves might be excited by narrow velocity spread electron beams as are believed to cause the similar upstream emissions. By comparing the voltages across antennas with different tip-to-tip lengths, Rodriguez [1979] concluded that the wavelengths of the magnetosheath turbulence exceeded 100 m across the entire frequency band from 40 Hz to 100 kHz. Since IMP 6 had a pair of orthogonal antennas and obtained the full waveform from 0 to 1.0 kHz, Rodriguez [1979] demonstrated that the electric field polarization in this frequency range was parallel to the magnetic field. At higher frequencies, Rodriguez and Gurnett [1975] used rapid sample (a measurement of a given frequency channel every 0.32 s) electric field amplitudes to show that the waves at 3.11 kHz were polarized along the field direction and stated that parallel polarization was a general property of the magnetosheath wave emissions.

Anderson *et al.* [1982] reported on two additional aspects of magnetosheath waves. Using the high time resolution capabilities of the ISEE 1 and 2 electric field spectrum analyzer and wideband system, Anderson *et al.* [1982] discussed short-duration emission spikes which spanned the frequency range from 100 Hz to 56 kHz. These spikes are a permanent feature of the nose region magnetosheath and made the main contribution to the spectral density above 1.0 kHz. The HAM passive sounder measurements indicated that the e -folding time of the spikes was less than or comparable to the 8-ms time constant of the HAM receiver. The electric field spectrum analyzer showed that the spikes occurred simultaneously at all frequencies within the 50 ms

Copyright 1993 by the American Geophysical Union.

Paper number 93JA02281.
0148-0227/93/93JA-02281\$05.00

NASA SCIENTIFIC AND TECHNICAL DOCUMENT AVAILABILITY AUTHORIZATION (DAA)

To be initiated by the responsible NASA Project Officer, Technical Monitor, or other appropriate NASA official for all presentations, reports, papers, and proceedings that contain scientific and technical information. Explanations are on the back of this form and are presented in greater detail in NHB 2200.2, "NASA Scientific and Technical Information Handbook."

Original
 Modified

(Facility Use Only)

Control No. _____

Date _____

I. DOCUMENT/PROJECT IDENTIFICATION (Information contained on report documentation page should not be repeated except title, date and contract number)

Title: Flux Solar Wind Interaction
Author(s): S. L. Moses and E. W. Greenstadt
Originating NASA Organization: NASA/GSFC

Performing Organization (if different) _____
Contract/Grant/Interagency/Project Number(s): NASA Grant 31216
Document Number(s): CR-189527 Document Date: _____

(For presentations or externally published documents, enter appropriate information on the intended publication such as name, place, and date of conference, periodical or journal title, or book title and publisher: _____
These documents must be routed to NASA Headquarters, International Affairs Division for approval. (See Section VII))

II. AVAILABILITY CATEGORY

Check the appropriate category(ies):

Security Classification: Secret Secret RD Confidential Confidential RD Unclassified

Export Controlled Document - Documents marked in this block must be routed to NASA Headquarters International Affairs Division for approval.

ITAR EAR

NASA Restricted Distribution Document

FEDD Limited Distribution Special Conditions-See Section III

Document disclosing an invention

Documents marked in this block must be withheld from release until six months have elapsed after submission of this form, unless a different release date is established by the appropriate counsel. (See Section IX)

Publicly Available Document

Publicly available documents must be unclassified and may not be export-controlled or restricted distribution documents.
 Copyrighted Not copyrighted

1N-93-CR
HCIT
140333
P. 36

III. SPECIAL CONDITIONS

Check one or more of the applicable boxes in each of (a) and (b) as the basis for special restricted distribution if the "Special Conditions" box under NASA Restricted Distribution Document in Section II is checked. Guidelines are provided on reverse side of form.

a. This document contains:

Foreign government information Commercial product test or evaluation results Preliminary information Information subject to special contract provision
 Other—Specify _____

b. Check one of the following limitations as appropriate:

U.S. Government agencies and U.S. Government agency contractors only NASA contractors and U.S. Government agencies only U.S. Government agencies only
 NASA personnel and NASA contractors only NASA personnel only Available only with approval of issuing office: _____

IV. BLANKET RELEASE (OPTIONAL)

All documents issued under the following contract/grant/project number _____ may be processed as checked in Sections II and III.

The blanket release authorization granted _____ is:

Rescinded - Future documents must have individual availability authorizations. Modified - Limitations for all documents processed in the STI system under the blanket release should be changed to conform to blocks as checked in Section II.

V. PROJECT OFFICER/TECHNICAL MONITOR

G. Bullock Office Code 602 Signature _____ Date _____
Typed Name of Project Officer/Technical Monitor

VI. PROGRAM OFFICE REVIEW

Approved Not Approved

Typed Name of Program Office Representative _____ Program Office and Code _____ Signature _____ Date _____

VII. INTERNATIONAL AFFAIRS DIVISION REVIEW

Open, domestic conference presentation approved. Export controlled limitation is not applicable.
 Foreign publication/presentation approved. The following Export controlled limitation (ITAR/EAR) is assigned to this document: _____
 Export controlled limitation is approved.

International Affairs Div. Representative _____ Title _____ Date _____

VIII. EXPIRATION OF REVIEW TIME

The document is being released in accordance with the availability category and limitation checked in Section II since no objection was received from the Program Office within 30 days of submission, as specified by NHB 2200.2, and approval by the International Affairs Division is not required.

Name & Title Tom Randall, Editorial Assistant Office Code 233.1 Date 5/24/94

Note: This release procedure cannot be used with documents designated as Export Controlled Documents, conference presentations or foreign publications.

IX. DOCUMENTS DISCLOSING AN INVENTION

a. This document may be released on _____ Date _____ Installation Patent or Intellectual Property Counsel _____ Date _____
b. The document was processed on _____ Date _____ in accordance with Sections II and III as applicable. NASA STI Facility _____ Date _____

X. DISPOSITION

Completed forms should be forwarded to the NASA Scientific and Technical Information Facility, P.O. Box 6767, B.W.I. Airport, Maryland 21240, with either (check box):

Printed or reproducible copy of document enclosed
 Abstract or Report Documentation Page enclosed. The issuing or sponsoring NASA Installation should provide a copy of the document, when complete, to the NASA Scientific and Technical Information Facility at the above listed address.